Developing a sequential cropping capability in the JULESvn5.2 land–surface model

Camilla Mathison[1,2], Andrew J Challinor[2], Chetan Deva[2], Pete Falloon[1], Sébastien Garrigues[3,4], Sophie Moulin[3,4], Karina Williams[1,5], and Andy Wiltshire[1,5]

[1]Met Office Hadley Centre, FitzRoy Road, Exeter, EX1 3PB, UK
[2]School of Earth and Environment, Institute for Climate and Atmospheric Science, University of Leeds, Leeds, LS2 9AT, UK
[3]EMMAH (UMR1114), INRA, Avignon, France
[4]Université d'Avignon et des Pays de Vaucluse, UMR1114 – EMMAH, 84000 Avignon, France
[5]School of, University of Exeter, Exeter, EX

Correspondence: Camilla Mathison (camilla.mathison@metoffice.gov.uk)

Abstract.

Sequential cropping (also known as multiple or double cropping) is common in tropical regions, where the crop seasons are largely dictated by the main wet season. The Asian summer monsoon (ASM) provides the water resources for crops grown for the whole year, thereby influencing crop production outside the ASM period. Land surface models (LSMs) typically simulate a single crop per year. However, in order to understand how sequential cropping influences demand for resources, we simulate all the crops grown within a year in a seamless way. In this paper we implement sequential cropping in a branch of the Joint UK Land Environment Simulator (JULES) and demonstrate its use at Avignon, a site that uses a form of the sequential cropping system. Avignon provides over 15-years of continuous flux observations which we use to evaluate JULES with sequential cropping. In order to implement the method in future regional simulations where there may be large variations in growing conditions, we apply the same method to 4-point simulations and a regional simulation for the North Indian states of Uttar Pradesh and Bihar to simulate the rice–wheat rotation and compare model yields to observations. The results show that JULES can simulate sequential cropping at Avignon, the four India locations and the regional run; representing both crops within one growing season in each of the crop rotations presented. At Avignon the maxima of leaf area index (LAI), above ground biomass and canopy height occur at approximately the correct time for both crops. The magnitudes of biomass, especially for winter wheat, are underestimated and the leaf area index is overestimated. The JULES fluxes are a good fit to observations (r values greater than 0.7), either using grasses to represent crops or the crop model, implying that both approaches represent the surface coverage adequately. For the India simulations, JULES successfully reproduces observed yields for the eastern locations; however, yields are under estimated for the western locations. This occurs in the regional simulation and the point simulations. This development is a step forward in the ability of JULES to simulate crops in tropical regions, where this cropping system is already prevalent. It also provides the opportunity to assess the potential for other regions to implement sequential cropping as an adaptation to climate change.

1 Introduction

Climate change is likely to impact all aspects of crop production affecting plant growth, development and crop yield (Hatfield and Prueger, 2015) as well as cropping area and cropping intensity (Iizumi and Ramankutty, 2015). The impact of climate change on agriculture has been the focus of several large collaborative projects such as the Agricultural Model Intercomparison and Improvement Project (AgMIP; Rivington and Koo, 2010; Rosenzweig et al., 2013, 2014) and the Inter-Sectoral Impact Model Intercomparison Project (ISIMIP; Warszawski et al., 2013, 2014). These projects have highlighted the likelihood of competition between crops grown for food and those grown for bio-energy in order to mitigate climate change (Frieler et al., 2015). Petrie et al. (2017) discuss how the use of sequential cropping systems may have made it possible for populations in some areas to adapt to large changes in monsoon rainfall between 2200–2100 BC. These ancient agricultural practices are common today across most tropical countries but may also be a useful adaptation, especially where traditionally mono-crop systems are currently used, in order to meet a future rising demand for food (Hudson, 2009) or the demand for bio-fuels. This sort of adaptation is already happening in some locations. Mueller et al. (2015) show that longer growing seasons in the extratropics have made the cultivation of multiple crops in a year at northern latitudes more viable. Warmer spring temperatures in the Brahmaputra catchment have allowed earlier planting of a winter crop, leaving time for a second crop (Zhang et al., 2013).

The South Asia economy is highly dependent on the agricultural industry and other industries also with a high demand for water (Mathison et al., 2015). The most important source of water for this part of the world is the Asian Summer Monsoon (ASM), which typically occurs between June and September (Goswami and Xavier, 2005); this phenomenon provides most of the water resource for any given year. The South Asia crop calendar is defined by the ASM which therefore has an important influence on the productivity across the whole year (Mathison et al., 2018) and therefore on crop production outside the Monsoon period.

Intercropping or sequential cropping allow farmers to make the most efficient use of limited resources and space in order to maximize yield potential and lower the risk of complete crop failure. These techniques also influence ground cover, soil erosion and chemical properties, albedo and pest infestation (Waha et al., 2013). Intercropping is the simultaneous cultivation of multiple crop species in a single field (Cong et al., 2015) while sequential cropping (also called multiple or double cropping) involves growing two or more crops on the same field in a given year (Liu et al., 2013; Waha et al., 2013). We use the term sequential cropping from here on to avoid confusion with other cropping systems. Sequential cropping systems are common in Brazil where the soybean–maize or soybean–cotton rotations are used (Pires et al., 2016) and for South Asia where the rice–wheat systems are the most extensive, dominating in many Indian states (Mahajan and Gupta, 2009), across the Indo-Gangetic Plain (IGP) (Erenstein and Laxmi, 2008) and Pakistan (Erenstein et al., 2008). States such as Punjab, Haryana, Bihar, Uttar Pradesh and Madhya Pradesh (Mahajan and Gupta, 2009) account for approximately 75 % of national food grain production for India. Rice-rice rotations are the second most prevalent crop rotation to rice-wheat rotations, these are typically found in the north eastern regions of India and Bangladesh (Sharma and Sharma, 2015) with some regions cultivating as many as three rice crops per year.

The modelling of crop rotations is a regular feature of soil carbon simulations (Bhattacharyya et al., 2007). Bhattacharyya et al. (2007) found that the rice–wheat rotation, common across the IGP, has helped maintain carbon stocks. However, in recent years, the yields of rice and wheat have plateaued, leading farmers to diversify and include other additional crops in the rotation, potentially depleting carbon stocks. The modelling of crop rotations has also been represented in the field of agricultural economics with work regarding sequential cropping being mainly to understand influences on decision-making; therefore focusing on short timescales and at the farm management level (Dury et al., 2012; Caldwell and Hansen, 1993).

Many dynamic global vegetation models (DGVMs), used to study the effects of climate change, simulate a single crop per year, both for individual sites and gridded simulations. This may be due in part to some global observation datasets such as Sacks et al. (2010) reporting only one growing period per year for most crops (Waha et al., 2012). Where different crop calendars are available for different regions e.g. MIRCA2000 (Portmann et al., 2010), rice and wheat are divided equally between the kharif (i.e. sown during the monsoon and harvested during the autumn) and rabi seasons (i.e. the drier winter/spring growing season), when in reality wheat is only grown during the rabi season (Biemans et al., 2016).

LPJml is one of the few models that is able to simulate sequential cropping. Sharma and Sharma (2015) use LPJml to simulate monoculture systems such as the rice–rice system grown in Bangladesh, while Waha et al. (2013) extend the Lund–Potsdam–Jena managed Land model (LPJml- Bondeau et al., 2007) to consider sequential cropping in Africa for two different crops. Waha et al. (2013) specify different growing season periods for each crop in the rotation, where the growing period is given by the sum of the daily temperatures above a crop specific temperature threshold. They also specify the onset of the main rainy season as the start of the growing season using the Waha et al. (2012) method. Waha et al. (2013) find that when considering the impact of climate change, the type of cropping system is important because yields differ between crops and cropping systems. Biemans et al. (2016) also use a version of LPJml, refined for South Asia, to estimate water demand and crop production for South Asia. Biemans et al. (2016) simulate sequential cropping by combining the output from two simulations with different kharif and rabi land-use maps and zonal sowing and harvest dates based on observed monsoon patterns. Biemans et al. (2016) find that accounting for the use of sequential cropping in this South Asia version of LPJml improved the simulations of the demand for water from irrigation, particularly the timing of the demand. The two main papers which try to simulate sequential cropping, Waha et al. (2013) and Biemans et al. (2016), have highlighted the importance of representing this cropping system in their simulations. It would be beneficial for more land-surface models to develop the capability to simulate different cropping systems and link crop production with irrigation both to improve the representation of the land surface in coupled models and to improve climate impacts assessments.

The JULES model is the land-surface scheme used by the UK Met Office for both weather and climate applications. It is also a community model and can be used in standalone mode; which is how it is used in the work presented here. The parametrisation of crops in JULES (JULES-crop) is described in Osborne et al. (2015) and Williams et al. (2017). JULES-crop is a dual-purpose crop model intended for use both within standalone JULES, enabling a focus on food production and water availability applications, as well as being the land-surface scheme within climate and earth system models. JULES-crop has been used in standalone mode in recent studies such as Williams and Falloon (2015) and Williams et al. (2017). The aim is that these studies and this one, will lead to using JULES in these larger models to allow the feed-backs from regions with extensive croplands and irrigation systems, like South Asia, to have an effect on the atmosphere e.g. via Methane emissions from rice paddies or evaporation from irrigated fields (Betts, 2005).

We describe and demonstrate the development and implementation of sequential cropping in JULES. This is part of a larger project to develop simulations for South Asia to understand the integrated impacts of climate change (Mathison et al., 2015, 2018) using state of the art RCM projections (Kumar et al., 2013; Mathison et al., 2013). This will improve understanding of the impacts of climate change and how they affect each other. Sequential cropping provides clear added benefits for the following reasons:

- by providing a more realistic representation of the land surface in terms of land-cover and fluxes in sequential cropping regions; this is not possible in a model which is only able to simulate mono-cropping systems.
- improving simulations of water resources by allowing the climate to affect both the water and crops, while simultaneously allowing interactions between water and crops throughout the year.
- by providing the opportunity to investigate the impact of adopting sequential cropping for regions where it is not currently used.

The purpose of this study is to use a site in France and two states in India to illustrate and evaluate the method implemented in the JULES standalone model at version 5.2 for simulating crop rotations; both irregular rotations as at Avignon and the sequential cropping systems used in India. The method is summarized by Fig. 1 and described in Sect 3. We aim to show, using the site in Avignon (France) described in Garrigues et al. (2015, 2018), that the method is able to simulate the change from one crop to another within a single growing period and therefore provide a closer representation of the real land surface at Avignon than previously possible using the original (mono-)crop model. Avignon is chosen because it has been observed and documented over several years (2001 to 2014), growing a range of crops throughout this period. No equivalent site to Avignon has been found for South Asia. The continuous measurements of surface fluxes provided by the Avignon dataset are a unique resource for evaluating land surface models (LSMs) and for testing and implementing more irregular crop rotations in LSMs. Garrigues et al. (2015) use this dataset to evaluate LSM simulations of evapotranspiration using the interactions between soil, biosphere, and atmosphere scheme (ISBA) LSM (Noilhan and Planton, 1989) specifically, the version from Calvet et al. (1998); ISBA-A-gs. We focus on a two-crop-rotation between 2005 and 2012.

We implement the method in a tropical region where there is large variation in growing conditions, applying the same method to the North Indian states of Uttar Pradesh and Bihar to simulate the rice-wheat rotation for both a region and four points across these two states. These states are key producers of these crops using the sequential cropping system. The aim of these simulations is to demonstrate the method works for these more variable regions, simulating two realistic crops each year.

The paper is structured as follows, Section 2 describes the JULES model and the method for implementing the sequential cropping system in JULES is outlined in Sect. 3. The simulations are described in Sect. 4, the observations used in Sect. 5, the results in Sect. 6 and Sect. 7 provides the discussion. Conclusions are provided in Sect. 8.

2 Model description

JULES is a process-based model that simulates the fluxes of carbon, water, energy and momentum between the land-surface and the atmosphere. JULES represents both vegetation (including natural vegetation and crops) and non-vegetation surface types including; urban areas, bare soil, lakes, and ice. With the exception of the ice tile all these tiles can co-exist within a gridbox so that a fraction of the surface within each gridbox is allocated between surface types. For the ice tile a grid box must be either completely covered in ice or not (Shannon et al., 2018). JULES treats each vegetation type as a separate tile within a gridbox, with each one represented individually with its own set of parameters and properties, such that each tile has a separate energy balance. The model and the equations it is based on are described in detail in Best et al. (2011) and Clark et al. (2011). Prognostics such as leaf area index (LAI) and canopy height are therefore available for each tile. The forcing air temperature, humidity and windspeed are prescribed for the gridbox as a whole for a given height. Below the surface the soil type is also uniform across each gridbox (where the number of soil tiles is set to one). We use JULES-crop (Osborne et al., 2015; Williams et al., 2017) to simulate the crops in this study. The main aim of JULES-crop is to improve the simulation of land-atmosphere interactions where crops are a major feature of the land-surface (Osborne et al., 2015).

Photosynthesis in JULES-crop uses the same parameters and code as the natural Plant Functional Types (PFTs). There are two temperature parameters: T_{low} and T_{upp}; these define the upper and lower temperature parameters for leaf biochemistry and photosynthesis within JULES (Clark et al., 2011) and are used to calculate V_{cmax}, the maximum rate of carboxylation of Rubisco (unstressed by water availability and ozone effects with units of $\mathrm{mol\ CO_2\ m^{-2}\ s^{-1}}$) as defined in Clark et al. (2011) and reproduced here in Eq 1. V_{cmax} is an important component in two limiting factors for photosynthesis; the Rubisco-limited rate and the rate of transport of photosynthetic products; Equation 1 shows the relationship between V_{cmax} and temperature. Gross Primary Productivity (GPP) is used to describe the total productivity of a plant; this defines the gross carbon assimilation in a given time. Net Primary Productivity (NPP) is GPP minus plant respiration; NPP is used in the crop partitioning code and subsequently in the calculation of the yield in JULES.

$$V_{\mathrm{cmax}} = \frac{V_{\mathrm{cmax25}} f_{\mathrm{T}}(T_{\mathrm{c}})}{[1+e^{0.3(T_{\mathrm{c}}-T_{\mathrm{upp}})}][1+e^{0.3(T_{\mathrm{low}}-T_{\mathrm{c}})}]} \tag{1}$$

where f_{T} is the standard Q_{10} temperature dependence

$$f_{\mathrm{T}}(T_{\mathrm{c}}) = Q_{10_leaf}^{0.1(T_c-25)} \tag{2}$$

and V_{cmax25} is assumed to be linearly related to leaf nitrogen concentration $n_l(0)$

$$V_{\mathrm{cmax25}} = n_{eff} n_l(0) \tag{3}$$

where n_{eff} represents the scale factor in the V_{cmax} calculation (in units of $\mathrm{mol\ CO_2\ m^2\ s^1\ kgC(kgN)^{-1}}$) and $n_l(0)$ the top leaf nitrogen concentration (in units of $\mathrm{kgN\ (kgC)^{-1}}$).

The effective temperature (see Eq. 4) is the function that the model uses to relate air or leaf temperature to the cardinal temperatures that define a plant's development; these are the base temperature (T_b), maximum temperature (T_m) and optimum temperature (T_o) and are specific for each crop. Different models define their effective temperature function in different ways, for example Fig. 1 of Wang et al. (2017) provides a number of different possible definitions. The JULES definition described by Eq 4 is most similar to type 4 given in Wang et al. (2017). Type 4 increases gradually towards the optimum temperature with a steeper decline from the optimum to the maximum. Other functions have no decline or a flatter top which can have different effects on the development of the crop. In JULES the cardinal temperatures and the 1.5m tile (i.e. air) temperature (T) are used to calculate the thermal time i.e. the accumulated effective temperature (T_{eff}) to which a crop is exposed (Osborne et al., 2015). Table 3 summarizes the settings for these temperatures used in this analysis. The crop model integrates an effective temperature over time as the crop develops through these stages with the carbon partitioned according to the Development Index (DVI).

$$T_{eff} = \begin{cases} 0 & \text{for} \quad T < T_b \\ T - T_b & \text{for} \quad T_b \leq T \leq T_o \\ (T_o - T_b)\left(1 - \dfrac{T - T_o}{T_m - T_o}\right) & \text{for} \quad T_o < T < T_m \\ 0 & \text{for} \quad T \geq T_m \end{cases} \tag{4}$$

The DVI is a function of the thermal time since emergence, therefore DVI=-1 is sowing, 0 is emergence and 1 is flowering. Maturity and therefore harvest occurs at a DVI of 2 (Osborne et al., 2015) under standard growth conditions but may be harvested earlier in other situations in the model (Williams et al., 2017). In reality the maturity date and the harvest dates are not usually the same date. The integrated effective temperature in each development stage is referred to as the thermal time of that development stage (Eq. 4 and Osborne et al. (2015); Mathison et al. (2018)).

Crop development can also be affected by the length of the day. However, in these simulations, as in (Osborne et al., 2015), this effect is not included. The thermal time is then used to calculate the rate of crop development or rate of increase of the Development Index, described by Eq. 5.

$$\frac{dDVI}{dt} = \begin{cases} \frac{T_{\text{eff}}}{TT_{\text{emr}}} & \text{for} \quad -1 \leq DVI < 0 \\ \left(\dfrac{T_{\text{eff}}}{TT_{\text{veg}}}\right) & \text{for} \quad 0 \leq DVI < 1 \\ \frac{T_{\text{eff}}}{TT_{\text{rep}}} & \text{for} \quad 1 \leq DVI < 2 \end{cases} \tag{5}$$

where TT_{emr} is the thermal time between sowing and emergence, TT_{veg} and TT_{rep} are the thermal time between emergence and flowering and between flowering and maturity respectively. These are calculated either using a temperature climatology from the driving data and sowing dates from observations or using the method presented in Mathison et al. (2018) to create a reliable sowing and harvest dataset. The advantage of using the Mathison et al. (2018) method is that there is no missing data, which is often the case when using observed data. Whichever source of sowing and harvest dates are used, the aim is for the crop to reach maturity, on average by the harvest date. The sowing and harvest dates used in the simulations in this analysis are described in Sect. 4.

In order to simulate the characteristics of a typical sequential cropping location using JULES we have implemented modifications to both JULES-crop and the irrigation code. To simulate crops in sequence on the same gridbox, each crop must be completed cleanly so the second one can be sown accordingly. The use of a latest harvest date forces the harvest of the first crop regardless of whether it has reached maturity or not. The latestharvestdate is a safeguard built into the model, usually set to a date well after the expected harvest date. It would be expected that when working properly the first crop would be harvested well before this time and this safeguard should not be needed. However if it is used the user is alerted that the harvest has been triggered because the crop has not matured. The user therefore knows when the model is not working correctly and has some initial information that aids the investigation into the nature of any problem. Although its use has been tested prior to implementation, the latest harvest date was not needed in the simulations demonstrating this method here. The latestharvestdate safeguard is preferable to the simulation of a crop growing for an unrealistically long time and overlapping the next growing season. This is essential for the implementation of sequential cropping at a global or regional scale, where the model is forced to grow crops that are potentially unsuitable for a particular gridbox. This is more likely for global simulations, which typically simulate a restricted set of crop types and varieties. These modifications are controlled using the l_croprotate switch (see table 1). Therefore l_croprotate ensures the following:

- All crops are initialized at the start of a simulation so that they can be used later when they are needed within the crop rotation being modelled.

- If JULES is simulating a crop rotation, the user must supply a latest harvest date so that the first crop is harvested before the second crop is sown (a latest harvest date can also be specified without using l_croprotate).

The current JULES default for irrigation allows individual tiles to be specified (when frac_irrig_all_tiles is set to false) but the irrigation is applied as an average across a gridbox and therefore actually occurs across tiles. The flag set_irrfrac_on_irrtiles restricts the irrigation to the tiles specified by irrigtiles only (see table 1). This new functionality is needed because many locations that include crop rotations include crops that both do and do not require irrigation.

3 Method for sequential cropping in JULES

The sequential cropping method implemented into JULES as part of this study is illustrated by the flow chart in Fig. 1 and described here using the Avignon site simulation. The Avignon site is a point run which is assumed to be entirely used to grow sorghum (from spring – late summer) and winter wheat (from winter – early summer). JULES updates the fraction of the site that is allocated to sorghum (winter wheat) just before the sowing date so that the appropriate crop occupies the whole of the site. The fraction of the site that is sorghum (winter wheat) is prescribed in the Avignon case using observed sowing and harvest

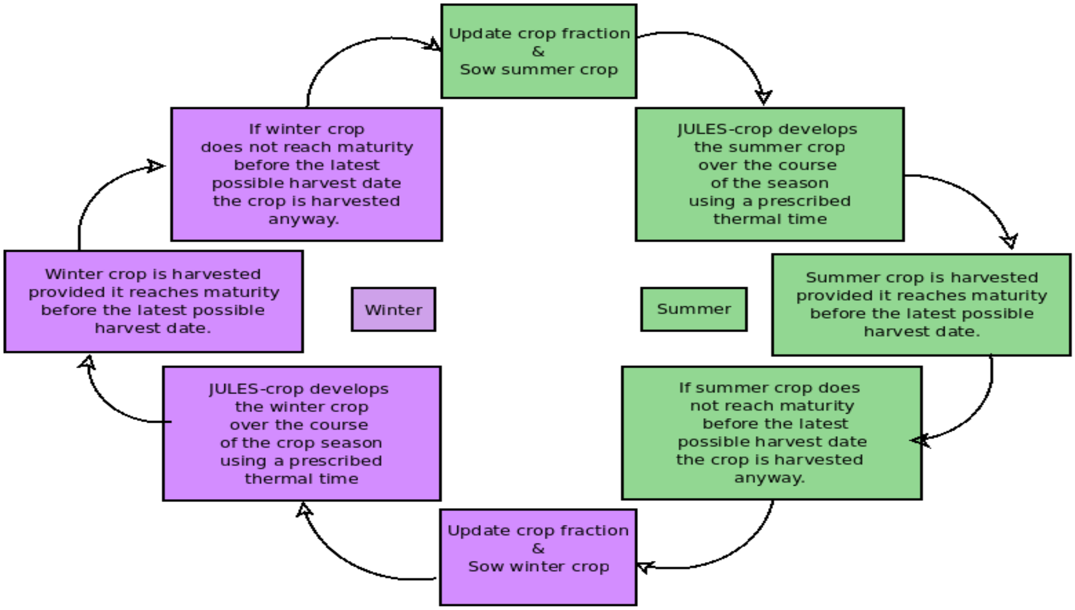

Figure 1. A flow chart showing the sequence followed to carry out the crop rotation in JULES. The first step (top green box) in the sequence is to update the first crop fraction, this occurs as or just before the first crop is sown.

dates. Once the fraction is updated the crop is sown, it then develops between the stages of: sowing and emergence, emergence and flowering and flowering and maturity.

It is recommended for sequential cropping to prescribe a latest possible harvest date for those instances where the crop does not develop quickly enough and therefore does not reach maturity before the next crop in the rotation is due to be sown (Sect. 2). In this study the latestharvestdate is set but never actually required for any of the simulations, which is the ideal scenario. The flow chart shown in Fig. 1 is equally applicable to the India simulations. Rice is therefore represented by the summer crop (green boxes) and wheat is represented by the winter crop (purple boxes). This method could be extended to include as many crops as occurs in a rotation at a particular location.

4 Model simulations

The description of the simulations is divided into two sections. Section 4.1 presents how the method is applied to a well observed site in order to describe and demonstrate how the cropping method works and evaluate it against observations at this location. The cropping system at the Avignon site is representative of a sequential cropping system, with sorghum planted during the summer months, followed by a winter wheat crop straight after. However, this site also represents a more irregular cropping pattern during some years, with a long fallow spell after the wheat crop and sorghum sometimes not sown until the following year. Section 4.2 applies the method to locations in Northern India where a more traditional sequential cropping system is commonly used, with a regular rotation between rice during the wetter kharif season and wheat during the drier rabi season. The parameter settings and switches used in JULES for the simulations in this study are provided in tables 1, 2 and 3. The Avignon and India simulations use the same settings wherever possible; these are provided in Table 1 (see Avignon settings and India settings columns). The nitrogen cycle in JULES cannot yet be used with the crop model so in these simulations, the same assumption is made as in Williams et al. (2017), that these crops are not nitrogen limited.

The plant functional type (PFT) parameter settings are also broadly the same between simulations, with the majority of these from Osborne et al. (2015) and therefore based on natural grasses. The crops are different between the two sets of simulations with winter wheat and sorghum at the Avignon site and spring wheat and rice at the India locations. The PFT parameters used in this study that govern V_{cmax}: including the lower (T_{low}) and upper (T_{upp}) temperatures for photosynthesis, n_{eff} and $n_l(0)$ are tuned to the maximum leaf assimilation expression from Penning de Vries et al. (1989) (see Table 2) for each crop. These values are consistent with the wider literature (Hu et al., 2014; Sinclair et al., 2000; Olsovska et al., 2016; Xue, 2015; Makino, 2003; Ogbaga, 2014). The parameters, μ_{rl} and μ_{sl} are the ratios of root to leaf and stem to leaf nitrogen concentrations respectively; these are tuned to those given in Penning de Vries et al. (1989) to lower the plant maintenance respiration, which was high in some of the initial simulations. The crop parameters are mainly from Osborne et al. (2015), with maize parameters used for sorghum (see Sect 4.1) except for the cardinal temperatures (see Table 3) which are from Nicklin (2012).

The calculation of the soil moisture availability factor (see Table 2) is different between the Avignon and India simulations. In the Avignon simulations we assume a rectangular root distribution and the total depth of the rootzone d_r to be 1.5 m, equivalent to the observed average maximum root depth over all of the years at the Avignon site. The soil moisture availability factor is then calculated using this maximum root depth together with the average properties of the soil. The India point simulations assume an exponential root distribution with an e-folding depth d_r of 0.5 m because we do not have an observed root depth for these locations. In all simulations in this study, we adjust the parameters that affect the use of water by the plant so that the plants experience less water stress (this parameter is P0 and is set to 0.5 (Allen et al., 1998), see table 2). This is because water stress is not the main focus of this analysis, but the representation of soil moisture stress on vegetation is a known issue in JULES; this is the subject of a large international collaborative effort (Williams et al., 2018; Harper et al., in preparation). The individual simulations are described in more detail in Sect. 4.1 and Sect. 4.2 for the Avignon and India simulations respectively. The purpose of including Avignon is because it provides a wealth of observations for evaluating Land surface models, where there is no equivalent site for South Asia. Observations of these fluxes show that the model is correctly representing the fluxes and coverage of the land surface. The purpose of including a simulation that does not use the crop model but approximates crops using grasses is to show how the model performs with the correct LAI and height i.e. it is a clean test of the representation of leaf photosynthesis, stomatal conductance, water stress and leaf-to-canopy scaling within the model (these parts of the code are shared by both natural vegetation and crops).

4.1 Avignon site simulation

The Avignon "remote sensing and flux site" of the National Institute Agronomic Research (INRA) described in Garrigues et al. (2015, 2018), provides a well studied location (France; 43°55’00.4"N, 4°52’41.0"E) with several years of crop rotation data. We focus on the period with a rotation of just two crops: winter wheat and sorghum between 2005 and 2012. The aim of simulating the crops at this site is to illustrate that the new sequential cropping functionality in JULES can simulate the change from one crop to another within a year and reproduce the correct growing seasons for each crop. JULES already contains parameterizations for wheat and maize. The wheat in JULES is the spring variety which is similar to the winter wheat crop that is grown at Avignon. Spring wheat does not require a vernalization period, which is a process usually needed for winter wheat varieties to achieve optimum yields (Griffiths et al., 1985; Robertson et al., 1996; Mathison et al., 2018). Vernalization is not explicitly implemented in JULES; therefore spring and winter wheat can be simulated interchangeably. The maize crop is a C4 crop that is similar to sorghum. Therefore we use these existing parameterizations rather than develop new ones. We evaluate JULES with sequential crops and grasses representing crops against the observed fluxes.

The Avignon JULES simulation (referred to from here on using AviJUL) is driven using the meteorological site observations outlined in Section 5.1 and Garrigues et al. (2015, 2018) using a half hourly timestep. Irrigation is only applied to the summer crops, this is the sorghum crop at Avignon. The observed irrigation amounts are added to the precipitation driving data at the exact day and time they were applied to the crops (Garrigues et al., 2015, 2018). The irrigation and other settings governing irrigation are therefore not switched on in JULES for the Avignon site simulations (See Table 1, column 'Avignon settings'). We include simulations for the Avignon site where the crops are represented by grasses (AviJUL-grass) for comparison with the simulations that use the new sequential cropping method implemented in the JULES-crop model (AviJUL-sqcrop). In the AviJUL-grass simulations the LAI and the canopy height are prescribed from observations in order to capture the growing seasons correctly without the crop model and the PFT parameters are adjusted to be the same as the crops. These AviJUL-grass simulations use the same photosynthesis and respiration calculation as JULES-crop in the AviJUL-sqcrop simulation, but this is not allowed to influence LAI as they do in the crop model. This allows the evaluation of the photosynthesis and respiration parts of the model, together with the water and energy fluxes, when the observed LAI and canopy height is used. In the AviJUL-grass simulations the JULES is not modelling the crops as grasses but fixing some parts of the crops (LAI and canopy height) straight to observations. In the AviJUL-sqcrop simulations the LAI and the canopy height are calculated by the model. Observed sowing and harvest dates from Garrigues et al. (2015) are used to calculate the thermal time requirements for each crop, these are provided in Table 4. During the periods between each crop, the ground is mostly bare (Garrigues et al., 2018).

4.2 India simulations

The India simulations focus on the north Indian states of Uttar Pradesh and Bihar. We include both point and a regional simulation for these states of India to demonstrate the method working for a true sequential crop rotation and a region. These states are key producers of rice and wheat in South Asia with the rice-wheat rotation prevalent in this part of India (Mahajan and Gupta, 2009). The sequential cropping system in this region involves growing rice during the wet monsoon months and an irrigated wheat crop during the dry winter. The wheat varieties grown in India are spring wheat, which is the standard variety represented by JULES (see Sect. 4.1). We select four points across these two states in order to gain understanding of the model response, particularly in terms of yield, to the variation in the conditions across the two states. The point simulations allow a similar type of analysis to the Avignon site while the regional simulation is useful for showing how this sequential cropping method will work for regional simulations.

The locations of the selected points are shown on a map of the surface altitude for South Asia in Fig. 2a. The driving data used for these four point simulations is from an RCM simulation run for South Asia for the period 1991–2007 as described below. Figure 2 (b, c and d) show a close-up view of the locations selected. Map (b) in Fig. 2 shows the average total monsoon precipitation for the 1991-2007 period while (c) and (d) show the average minimum and maximum temperatures respectively to illustrate that these four points are representative of the climate of the wider Uttar Pradesh/Bihar region.

In both the point and regional simulations JULES is run using a 3-hourly timestep using driving data from ERA-interim (Dee et al., 2011; Simmons et al., 2007) downscaled to 25 km using the HadRM3 regional climate model (RCM- Jones et al., 2004). This RCM simulation is one of an ensemble of simulations produced for the EU-HighNoon FP7 project for the whole of the Indian subcontinent (25 N, 79 E–32 N, 88 E) for the period 1991-2007. The HighNoon simulations are described in detail in previous publications such as Kumar et al. (2013) and Mathison et al. (2013, 2015). HadRM3 provides more regional detail to the global data with lateral atmospheric boundary conditions updated 3-hourly and interpolated to a 150 s timestep. These simulations include a detailed representation of the land surface in the form of version 2.2 of the Met Office Surface Exchange Scheme (Essery et al., 2001, MOSESv2.2;). JULES has been developed from the MOSESv2.2 land surface scheme and therefore the treatment of different surface types is consistent between the RCM and JULES (Essery et al., 2001; Mathison et al., 2015). In the India point simulations the sowing dates are prescribed using climatologies calculated from the observed dataset, Bodh et al. (2015), from the government of India, Ministry of Agriculture and Farmers welfare. Thermal times are calculated using these climatological sowing and harvest dates from Bodh et al. (2015) and a thermal climatology from the model simulation as described in Osborne et al. (2015), the values used in the simulations here are provided in Table 5. In the regional simulation the thermal time requirements are estimated from the sowing and harvest dates provided by the Mathison et al. (2018) method to avoid problems with missing observed data. Only wheat is irrigated in these India simulations (both point and regional), the settings used for these are provided in Table 1 (column 'India settings'). Plots of the regional ancillaries for each of rice and wheat are provided in Appendix C.

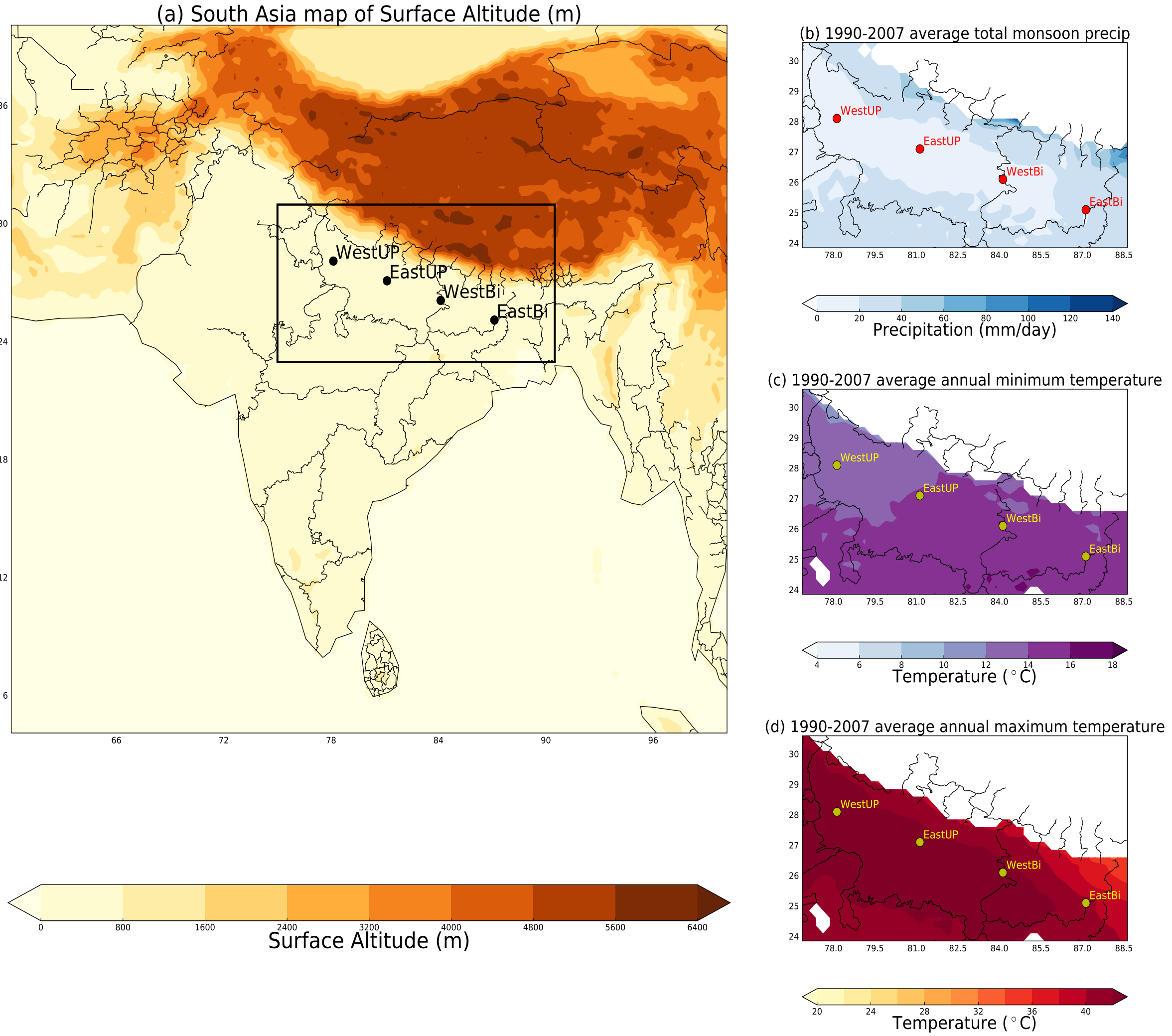

Figure 2. A map showing the location of the point simulations in the wider context of India on a map of the surface altitude (a) from the regional climate model that is used in the JULES simulations. The same points are shown in three smaller maps (b,c,d) that zoom in on the two states of Uttar Pradesh and Bihar. Map (b) shows the total monsoon precipitation, map (c) shows the minimum temperature, and map (d) the maximum temperature averaged for the period 1991-2007.

5 Observations

5.1 Avignon observations

The length and detail of the observation record at the Avignon site means it is an ideal site to demonstrate the method being implemented in JULES for simulating sequential cropping. High resolution meteorological data, important for the practicalities of running the JULES model is available on a half hourly basis; this includes air temperature, humidity, windspeed and atmospheric pressure at a height of 2m above the surface. Cumulative rainfall, radiation measurements and sensible (H) and latent heat (LE) fluxes are also available, with the latter flux measurements enabling the evaluation of the JULES fluxes. Cumulative evapotranspiration (ET) are derived from the half hourly LE measurements. The observations for evaluating the model include soil measurements of soil moisture along with plant measurements including canopy height (measured every 10 days), above ground dry weight biomass (taken at four field locations) and LAI; biomass and LAI are destructive measurements repeated up to six times per crop cycle (Garrigues et al., 2015). More information is documented in Garrigues et al. (2015) regarding the site and the observations available.

5.2 India observations

Crop yield observations from the International Crops Research Institute for the Semi-Arid Tropics (ICRISAT, 2015) provides seasonal yields for each crop for each district for comparison with the point simulations. We also show average crop yield observations for three, 5-year periods between 1993 and 2007 (1993–1997, 1997–2003, 2003–2007) (Ray et al., 2012a). Data from Ray et al. (2012a) is made available via Ray et al. (2012b). Ray et al. (2012b) are based on previous publications Monfreda et al. (2008) and Ramankutty et al. (2008). All the observations used include the period of the point simulations which are from 1991–2007. We show both of these datasets to highlight that there is a range in the estimates of yield for this region.

6 Results

6.1 Avignon site results

Avignon is characterized by a Mediterranean climate with a mean annual temperature of 287.15°K (14°C and most rainfall falling in autumn (with an annual average of 687 mm). The Avignon timeseries of temperature (with a 10-day smoothing applied) is shown in Figure 3a and precipitation (10-day totals, which include actual irrigation amounts) in Fig. 3b (Garrigues et al., 2015). Figure 3 shows the fairly regular distribution of rainfall throughout the year (b) and the relative consistency of the annual temperature range for Avignon (26°), with only a brief cold snap in early 2012 having a much lower minimum.

Figure 4 shows the timeseries of total above ground biomass (a), LAI (b) and canopy height (c) for the AviJUL-sqcrop simulations. AviJUL-grass are also shown in Fig 4, however these follow the observed canopy height and LAI exactly as these values are prescribed in the simulations without crops. Figure 4 shows that the crops are developing throughout the crop seasons with maxima of biomass, LAI and canopy height occurring at approximately the correct time for both crops. This

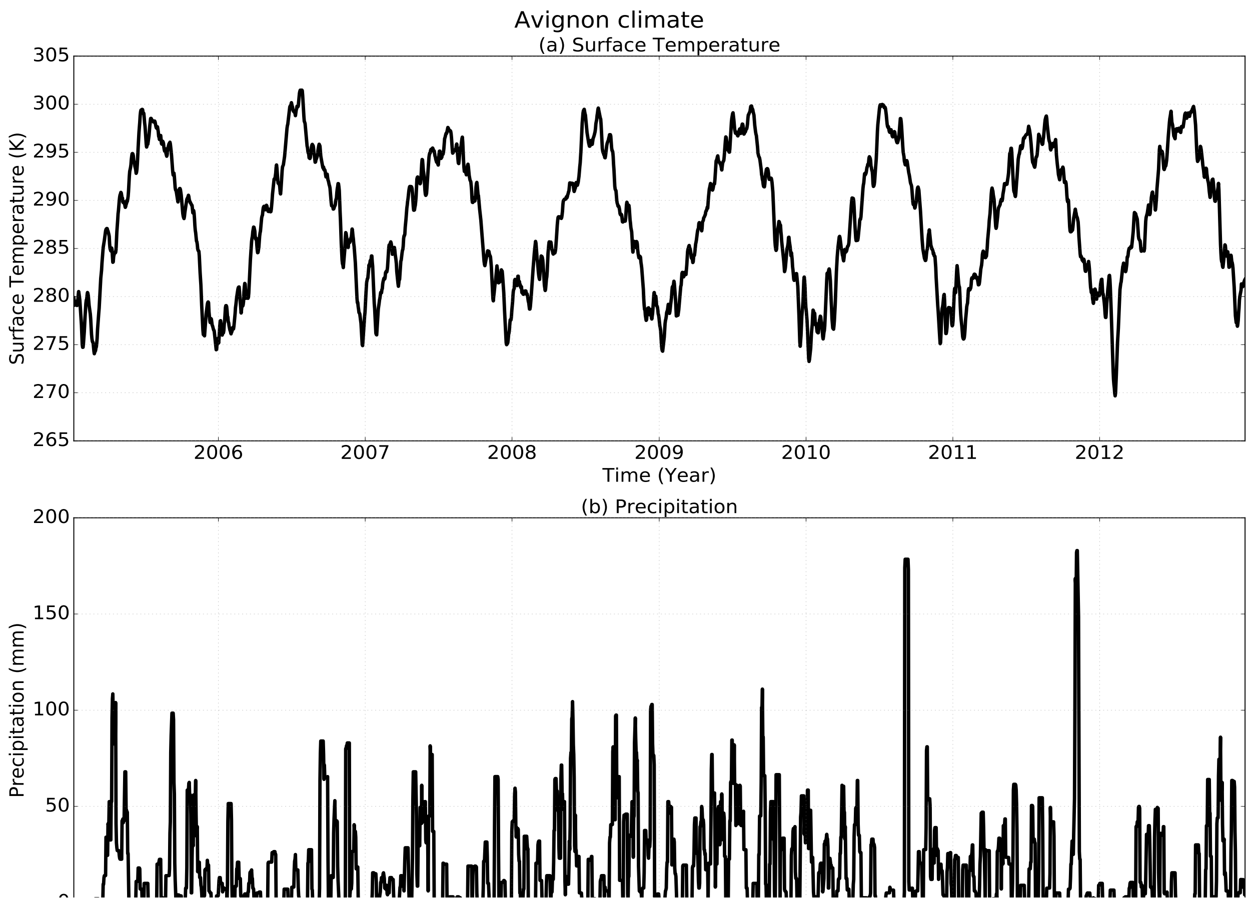

Figure 3. Timeseries of temperature (a) and precipitation (b) at Avignon for the time period analysed (2005-2012)

shows that the lack of vernalization in the model does not affect the simulation of winter wheat at Avignon. The total above ground biomass from JULES is calculated from the sum of the stem, leaf and harvest carbon pools for each crop and plotted as a time series (dashed lines). Biomass observations are provided as a single timeseries with the crop type confirmed from the timing of the observations. These are plotted alongside the model represented by purple asterisks (Fig. 4a).

The observed growing season for sorghum in 2009 is much shorter than for the other two sorghum crop seasons (shown by the red solid line in Fig. 4 b and c). The 2009 sorghum crop is planted much later in the year compared to the other two sorghum seasons (2007 and 2011) but harvested at a similar time. This is because the variety of sorghum planted in 2009 is different to the variety planted 2007 and 2011 seasons. The 2009 variety is a fodder crop with a much larger LAI and a shorter growing season.

JULES fits the biomass observations for 2009 well (Fig. 4a). JULES also closely fits the LAI (Fig. 4b) and canopy height observations (Fig. 4c) for the 2009 Sorghum season, with differences between the simulations and observations maximum values of approximately $1\ \mathrm{m}^2\ \mathrm{m}^{-2}$ and $0.1\ \mathrm{m}$ respectively. In the 2007 sorghum season JULES overestimates the maximum

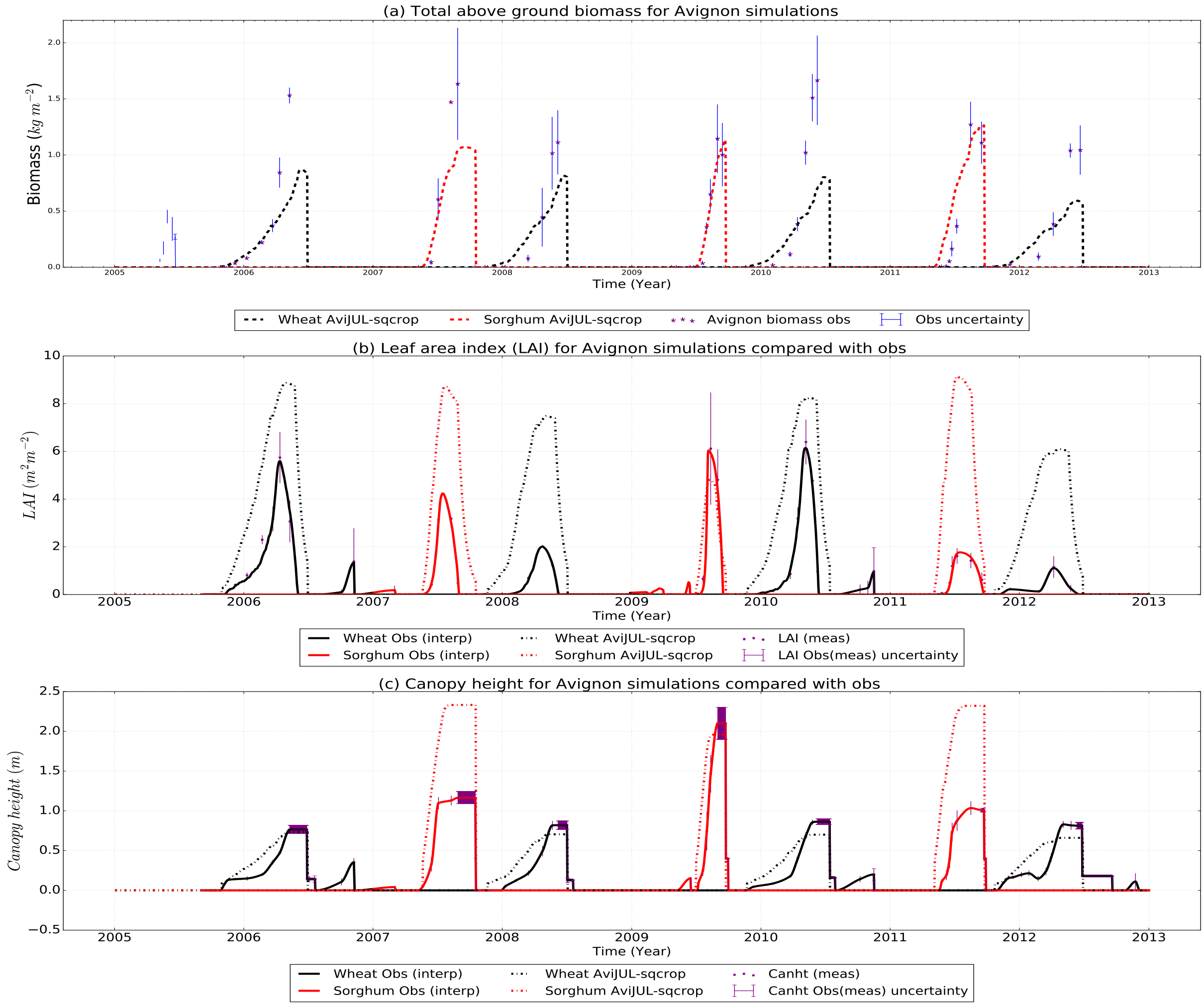

Figure 4. Timeseries of total above ground biomass (a), leaf area index (LAI) (b) and canopy height (c) for the Avignon site for wheat (black) and sorghum (red) for observations (solid lines) and simulations using the observed sowing and harvest dates: AviJUL-sqcrop and modelled soil moisture (dashed) for the period between 2005 and 2013 using observed sowing and harvest dates. Simulations with prescribed LAI and canopy height are not shown here as these follow the observed LAI and canopy height. Observed above ground biomass in plot (a) shown by purple asterisks. The standard deviation of the measurements is shown to represent the uncertainty in the observations

LAI and canopy height by approximately two times the observations (see Fig. 4b and c) and underestimates the total biomass (see Fig. 4a) by about 30 %. For the 2011 season the JULES sorghum biomass equals the magnitude of the observations; however, the maximum LAI is overestimated by four times in the model (similar to 2007) and the maximum canopy height is approximately two times the observed maximum. The canopy height is very close to observations for wheat in all four seasons;

however, the wheat LAI is overestimated and the biomass is underestimated in all years. The two wheat seasons of 2006 and 2010 are closer to the LAI observations than 2008 and 2012, but the underestimation of the biomass is greater for these seasons. The increase in biomass for both crops through the start of the season follows the observations quite closely but in most years, especially for wheat, JULES does not accumulate enough biomass later in the crop season to reach the observed maxima.

The peaks in productivity shown in the LAI in Fig. 4b are consistent with the two years (2006 and 2007) of GPP observations, shown by the black line in Fig. 5a. The wheat crop is clearly shown in the GPP for 2006, although it is underestimated in all simulations (Fig. 5a). The decline in GPP at the end of the 2006 wheat season is quite close to the observations for both simulations, with AviJUL-grass (red line) being slightly early and AviJUL-sqcrop (blue line) being slightly late. In the 2007 sorghum season the magnitude and timing of the maximum GPP for AviJUL-sqcrop (blue line) are a good fit to observations, although the increase in GPP begins slightly too early for AviJUL-sqcrop and slightly late for AviJUL-grass. The AviJUL-grass simulations slightly underestimate the maximum GPP during the sorghum season and it occurs a little later than observed (Fig. 5a). The decline in GPP at the end of the sorghum season occurs at the same time as the observations for both AviJUL-grass and AviJUL-sqcrop. These results are quantified in Fig. A.1 with both AviJUL-grass (a) and AviJUL-sqcrop (b) showing a strong linear correlation with r values of above 0.7 (Fig. A.1a and A.1b and the values in the GPP row of Table 6).

The H and LE fluxes are shown in Fig. 5b and Fig. 5c respectively. The AviJUL-sqcrop (blue line) and the AviJUL-grass (red line) simulations follow each other closely which is reflected in the RMSE values and bias values for each simulation (see Table 6 and Figures A.2 and A.3 for H and LE comparisons respectively), these are generally comparable to those from Table 5 in Garrigues et al. (2015), which are LE: rmse of 52.4 Wm^{-2}, bias of -11.8 Wm^{-2}, and H: rmse of 56.2 Wm^{-2}, bias of 17.6 Wm^{-2}. The linear correlations shown for H and LE in Fig. A.2 and Fig. A.3 respectively, are strong for these simulations with r values above 0.7, (grasses shown in a and sequential crop shown in b). These values are comparable to those from Table 5 in Garrigues et al. (2015), which provides correlation values of 0.8 for LE and 0.85 for H. The annual cycle of LE and H are shown in Fig. A.4, a and b respectively. Figure A.4 highlights how well the simulations capture the seasonal cycle; this is also evident in the timeseries shown in Fig. 5, plot b and c.

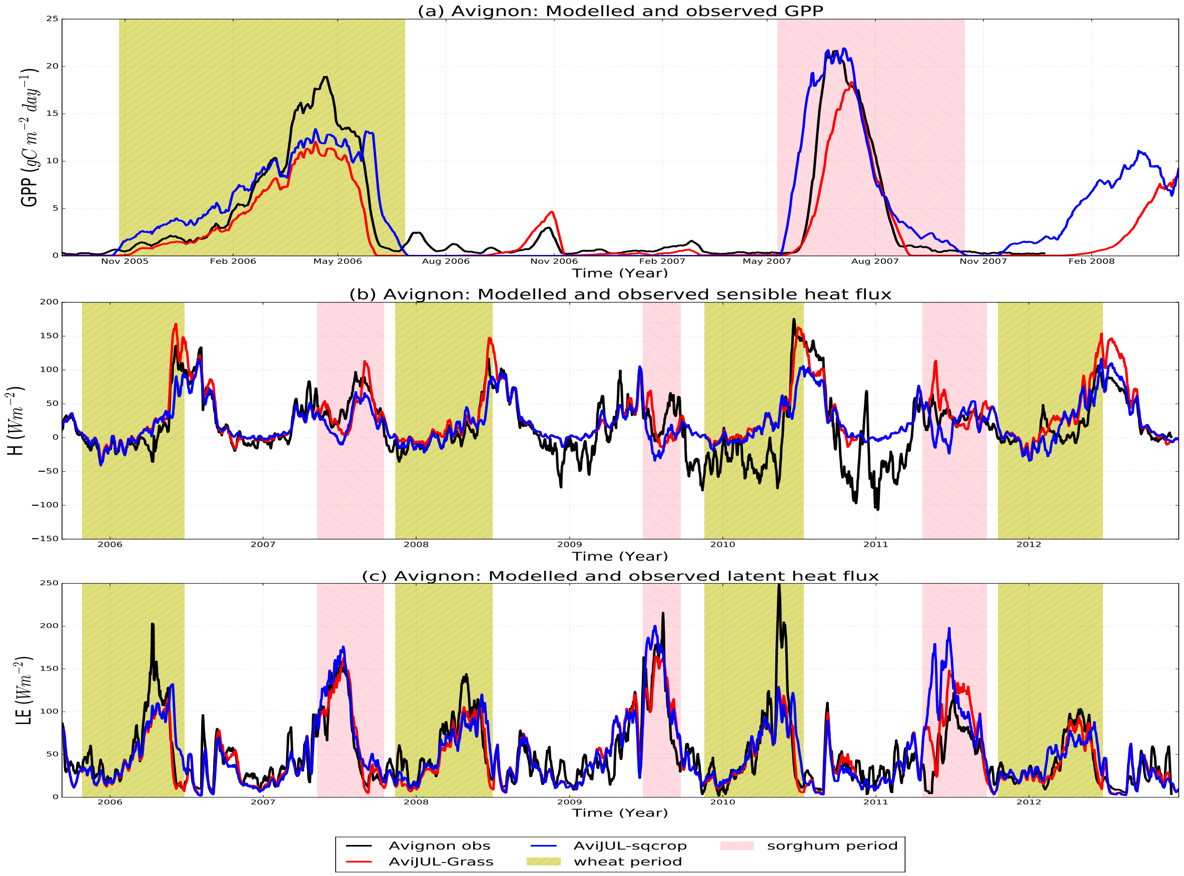

Figure 5. Timeseries of GPP (a), H (b) and LE (c) for the Avignon site compared with observations (black lines). H (b) and LE (c) heat fluxes show the whole period from 2005-2012, while GPP shows the period 2005-2008 due to availability of observations. In the GPP plot only one complete winter wheat (yellow) and one complete sorghum season (pink) are highlighted. The following model simulations are also shown: AviJUL-grass with prescribed LAI and modelled soil moisture (red), AviJUL-sqcrop with both soil moisture and LAI modelled (blue). In each plot a 10-day smoothing has been applied to the daily data.

6.2 India point results

The four India points selected for analysis in this study are shown on a map of South Asia in Fig. 2 (plot a) with smaller inset plots (b, c and d) focusing on the sequential cropping region being considered across the states of Uttar Pradesh and Bihar. Figure 6 shows the differences in the timeseries of the average precipitation (a), temperatures (b), and vapour pressure deficit (VPD) (c) at each of these four points with the different crop seasons emphasized by the different colour shading (yellow for wheat and pink for rice) on each of the plots. The temperatures rarely reach the low temperatures of the t_{base} cardinal temperatures set in the model shown for rice (green) or wheat (orange) on Fig. 6 (b); however the high temperatures do exceed the maximum cardinal temperatures for these crops, especially those set for wheat. In general EastBi is cooler than the other points in more of the years, with the two locations in Uttar Pradesh often being the warmest. The precipitation at each location is variable (see Fig. 6 plot a) with variation in the distribution of precipitation through the monsoon period which could be important for crop yields. Challinor et al. (2004), for example, found that in two seasons with similar rainfall totals, the distribution of the rainfall during the growing season strongly affected groundnut crop yield. There is also a clear seasonal cycle in the vapour pressure deficit (VPD), increasing toward the end of the wheat season and decreasing into the rice season. EastBi generally has the lowest VPD, with WestUP and EastUP usually the highest throughout the timeseries shown (see Fig. 6). These plots suggest that there is a gradual change in conditions from west to east across Uttar Pradesh and Bihar with increasing humidity and rainfall and decreasing maximum temperatures from west to east.

The sequential cropping simulations at these India locations produce both a rice and wheat crop yield (see Fig. B.1, with red representing rice and black representing wheat). JULES is therefore growing both wheat and rice at each of these locations within one growing season and is therefore simulating the sequential cropping rotation. We first consider if the main crop characteristics such as LAI and canopy height are realistic. This is important, especially where the results are to be applied to analysis of future water resource requirement, where an overestimation (underestimation) of size or leaf area for a crop could skew the results towards a higher (lower) resource requirement. In these simulations the canopy height (see Fig. B.3) for both rice and wheat at each location is between 0.5 and 0.7 m (see Fig. B.3) which is an expected value for a typical crop, as described in (Penning de Vries et al., 1989). Figure 8 shows the LAI for each of the four locations, indicating that the wheat LAI from JULES is between 5 and 7 $\mathrm{m^2 m^{-2}}$ across the locations; this is also an expected value for a crop according to Penning de Vries et al. (1989). Rice LAI is lower (between 2 and 4 $\mathrm{m^2 m^{-2}}$) with the lowest values for WestUP, slightly increasing from west to east locations. For WestUP particularly, rice (red solid line) has a small LAI (see Fig. 8) but it generates a yield (red asterisks Fig. B.1) that falls within the range of the observations for each year. However, wheat (black solid line) generates a LAI that is closer to expected values but a smaller yield compared with observations (see Fig. B.1, black asterisks).

Figure 7 shows the observed yields from ICRISAT (2015) compared against the model yields at each of the India locations. Figure 7 shows how the yields change at each of the locations from west to east. The observed yields, particularly for wheat are larger to the west reducing to the east. The model underestimates the western yields but tends to overestimate the eastern yields. This is confirmed in the timeseries of the harvest pool (solid lines) for each crop shown in Appendix B, Fig. B.1. Figure B.1 shows the model yield (asterisks), the average dataset from Ray et al. (2012a) (filled triangles) and the ICRISAT (2015)

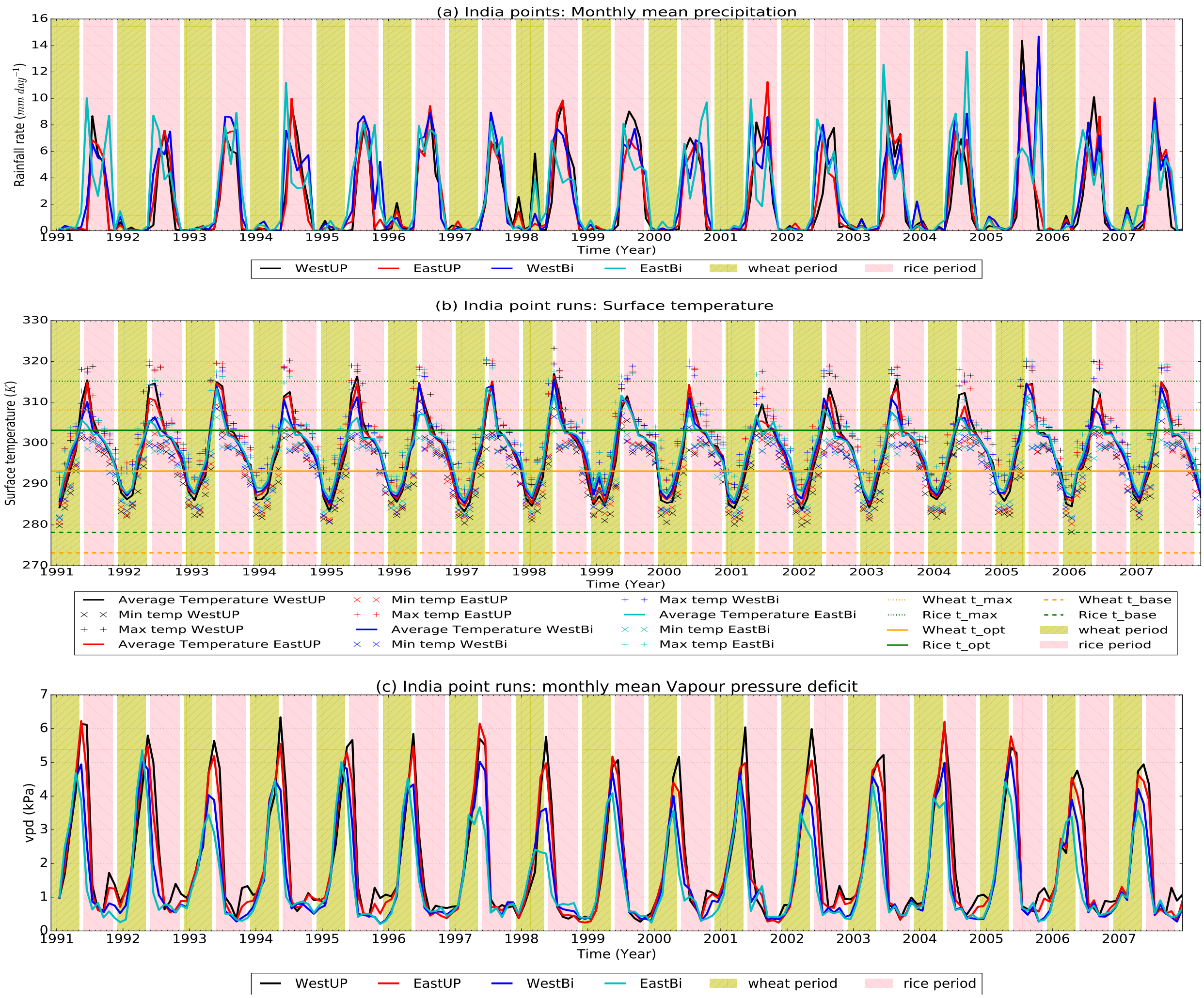

Figure 6. Timeseries of monthly precipitation (a), temperature (b), and vapour pressure deficit (c) at each of the India sites shown by the solid lines (WestUP-black, EastUP-red, WestBi-blue and EastBi-cyan). Plot (b) also shows the minimum ('x') and maximum ('+') temperatures for each of the locations for each month together with the JULES cardinal temperatures (horizontal lines) for rice (green) and wheat (orange): Max temperatures (dotted line), optimum temperatures (solid line) and base temperatures (dashed line).

yield (filled circles) (as on Fig. 7). The inclusion of both observation datasets highlights the spread between yield estimates for this region. At WestUP, (asterisks on Fig. B.1, Fig. 7 black circles) the average bias between the model and observations across both datasets is -0.13 $\mathrm{kg\ m^{-2}}$ for wheat and -0.064 $\mathrm{kg\ m^{-2}}$ for rice (Fig. 7 red circles). The average bias across both observation datasets is much smaller for the other locations with rice and wheat yields within the range of the observations for most years for both EastUP and WestBi (average bias across both crops at these locations ranges from -0.07 to 0.02 $\mathrm{kg\ m^{-2}}$).

During the second half of the simulation the wheat yield is underestimated by the model more often at EastUP but this is just the occasional year for WestBi and does not occur at all for EastBi. For EastBi the rice yields are often toward the top of the range provided by the two observed datasets but still within the range of the observations (see Fig. B.1); this gives on average a positive bias of 0.06 for rice and 0.02 for wheat.

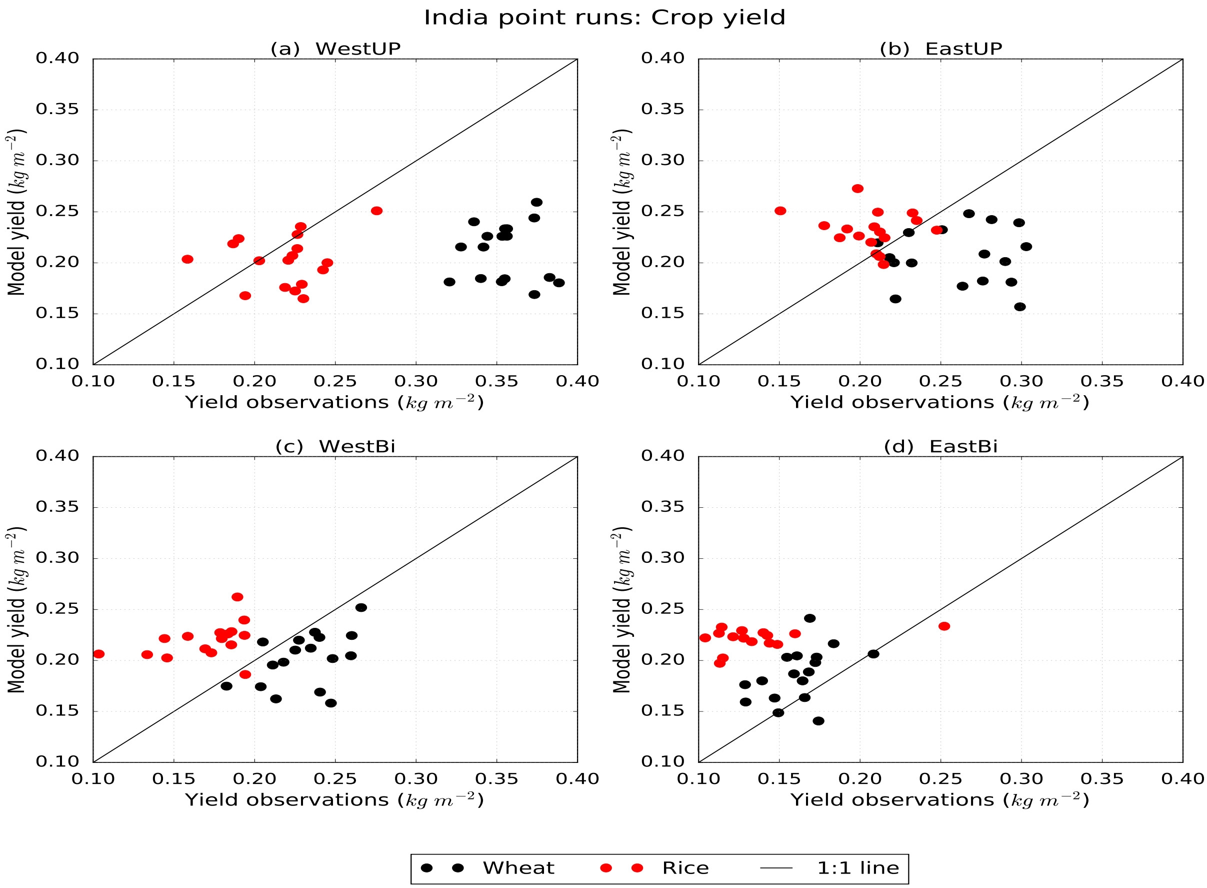

Figure 7. Scatter plot comparing the rice (red) and wheat (black) yields in the ICRISAT observations (ICRISAT, 2015) against those in the JULES simulations at each of the India sites shown in Fig. 2.

Figure.10c shows the annual climatology of NPP for each of the India locations, an annual timeseries is also shown in the Appendix B in Fig. B.4c. These show that Wheat NPP begins its decline too early in the wheat season (Fig.B.4c and 10c around day 41), which has a direct impact on the yield. This could be related to the way the carbon is partitioned to different parts of the plant or due to the ratio of thermal time of vegetation to reproduction in JULES. A short timeseries showing how carbon is partitioned to the different parts of the plant for wheat (black) and rice (red) are shown in Fig. 9. The relationship between NPP and the yield is discussed further in Sect. 7.2.

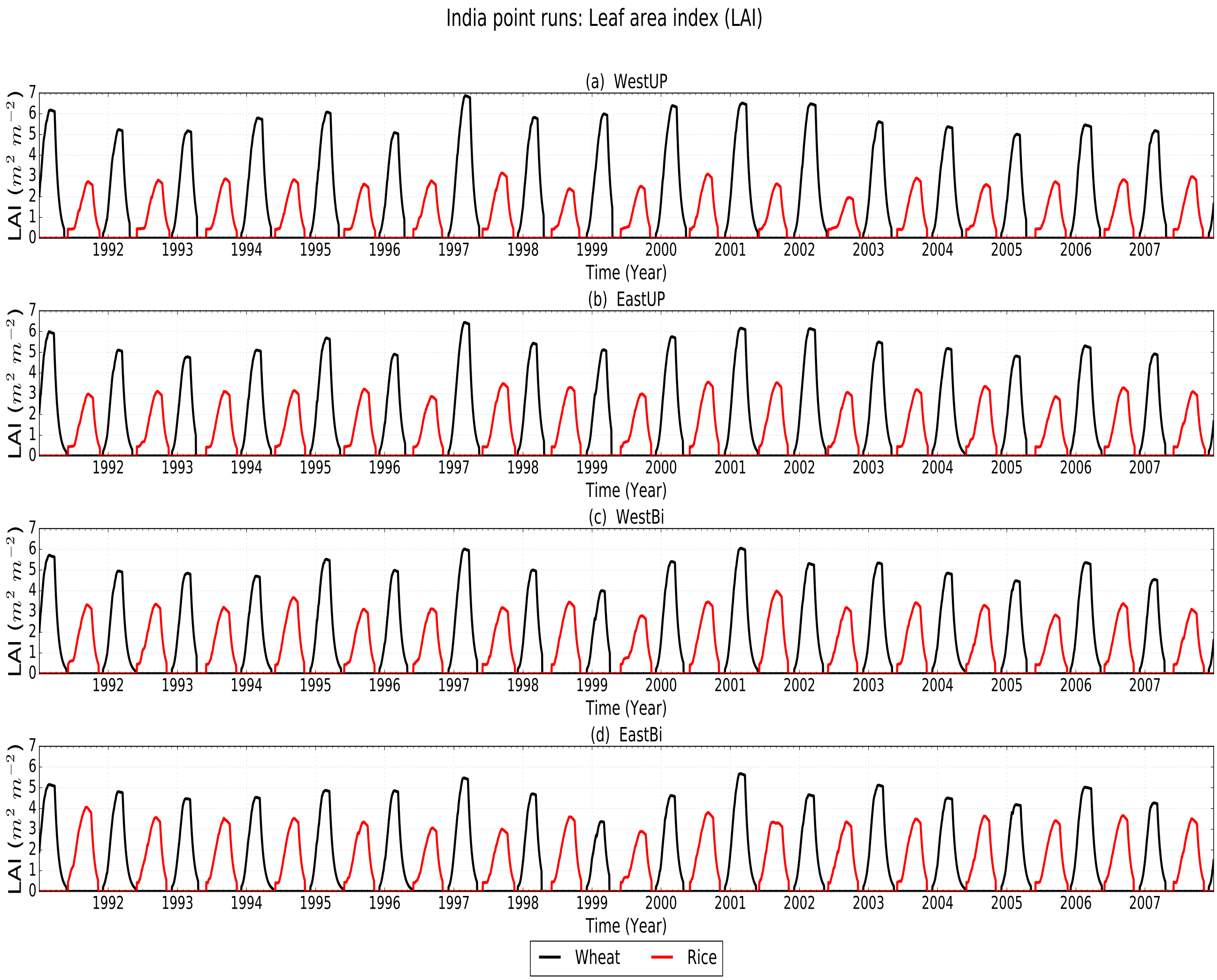

Figure 8. Timeseries of the leaf area index rice (red) and wheat (black) at each of the India sites shown in Fig. 2.

The fluxes of heat (LE and H), NPP and GPP are shown for each of the four India locations (identified on Fig. 2) as annual climatologies in Fig. 10 and timeseries of the whole simulation in Fig. B.4, Appendix B. They show the influence of the sequential crop rotation of wheat and rice on the fluxes at each location by the presence of a first peak for wheat and a secondary smaller peak during the rice season. This is most obvious in the plots of NPP and GPP (see Fig. 10 and Fig. B.4, plot (c) and (d) respectively). In general the timeseries and the annual cycles of the fluxes shown in Fig. 10 and Fig. B.4 are quite similar between locations, with minima and maxima occurring at the same time.

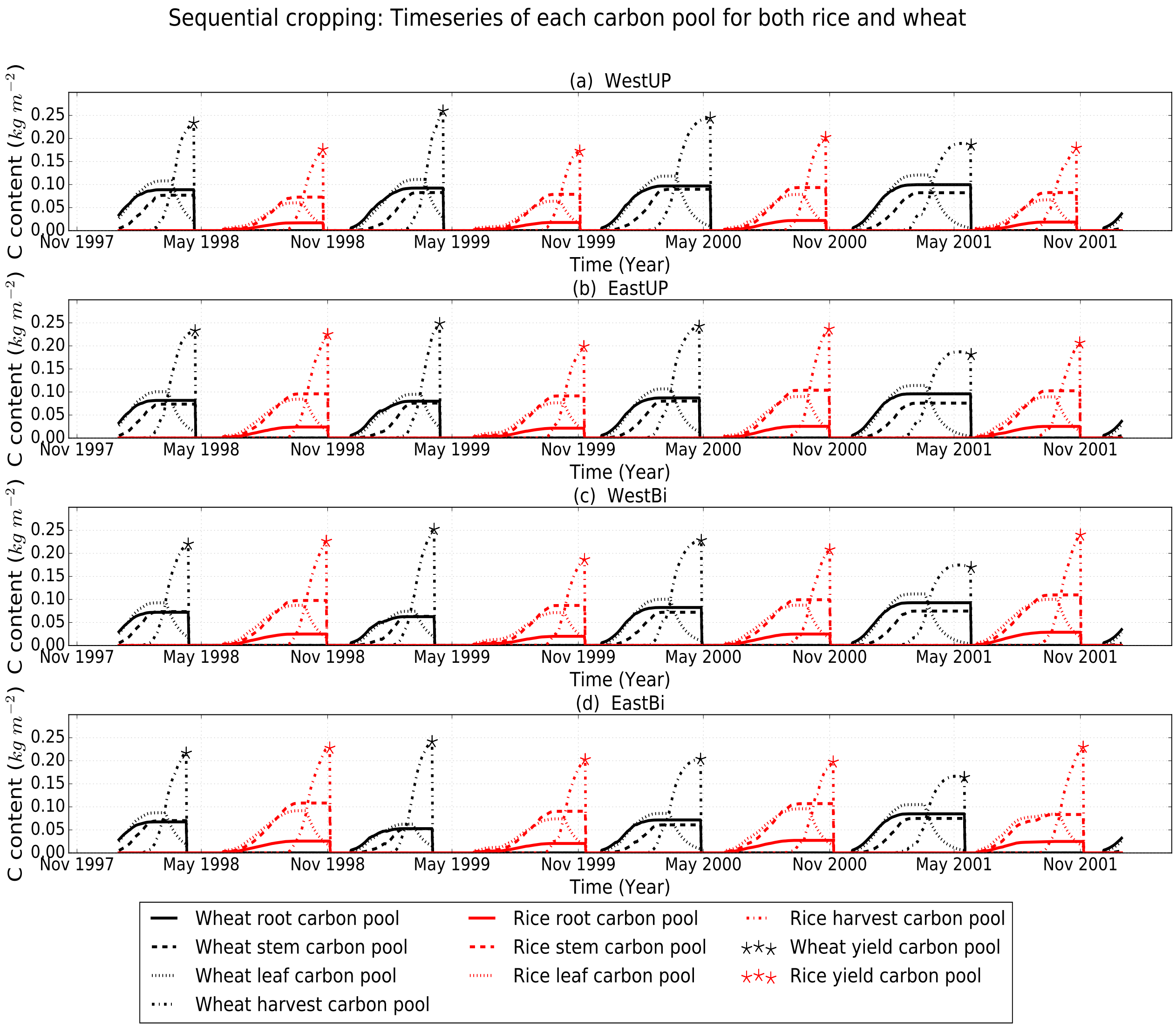

Figure 9. Timeseries of each crop carbon pool: leaf (solid lines), root (dashed), stem (dotted) and harvest (dash-dot) with the JULES yield at the time it is output by the model (asterisks) for rice (red) and wheat (black) at each of the India sites shown in Fig. 2 for a subset of years of the simulation between 1998 and 2001.

The drier hotter location, WestUP usually has a lower LE together with a higher H than the other three locations. There are two short periods in 1998 and 2001, where EastBi has the lowest available soil moisture, these periods correspond with a lower monsoon rainfall at this location (see Fig. 6). The available soil moisture in the top 1.0 m of soil and the soil moisture availability factor (Beta, β) are shown in Fig 11 and Fig. B.5, plot a and b respectively). β is based on the top 1.4m of soil, it is zero below the wilting soil moisture and one above a critical soil moisture, this is shown in Fig. 1 of Williams et al.

(2018). The annual timeseries of these moisture fields (Fig. B.5) shows that for several years of the simulation WestUP has the lowest available soil moisture and therefore β value, suggesting this location is likely to be the most water stressed. The annual climatology of these two moisture fields shows that the WestBi on the other hand often has the highest β and the most consistent available soil moisture in the top 1.0 m across the year of the four locations. This is consistent with the temperature and precipitation timeseries shown in Fig. 6 where the locations to the east are wetter and cooler than those to the west. This means there is more available soil moisture in the top 1.0 m for the eastern locations compared with the western locations.

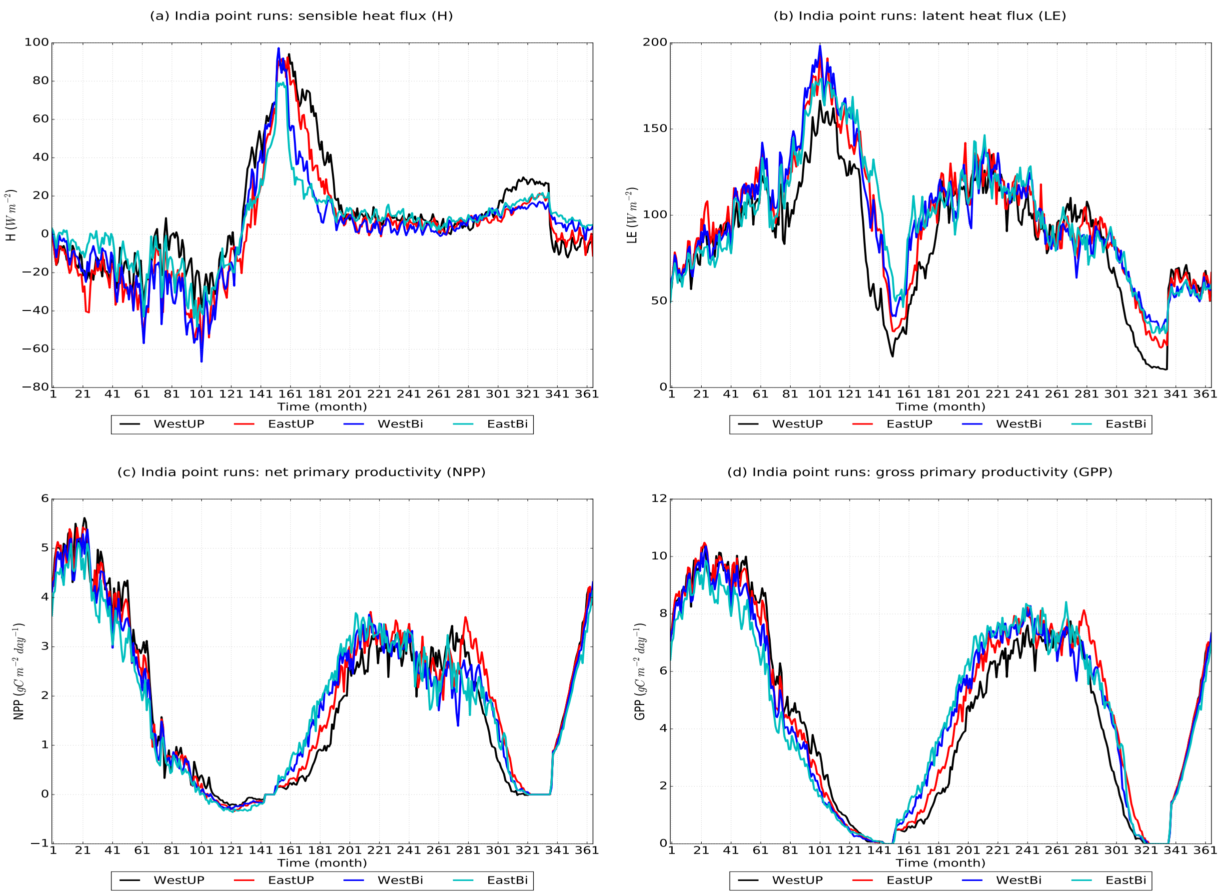

Figure 10. Annual climatology (in day of year) of H (a), LE (b), gridbox NPP (c) and gridbox gpp (d) at each of the India sites shown in Fig. 2. Each location is represented by a solid line of a different colour: WestUP - black, EastUP - red, WestBi - blue and EastBi - cyan

6.3 India regional results

Figures 12 and 13 show the average of the maximum annual LAI and canopy height for each crop for the regional simulation of the rice–wheat rotation across Uttar Pradesh and Bihar between 1991-2007. Similarly to the point simulations, the canopy heights are quite large for both rice and wheat, while the LAI is smaller, particularly for rice and to the west of the region.

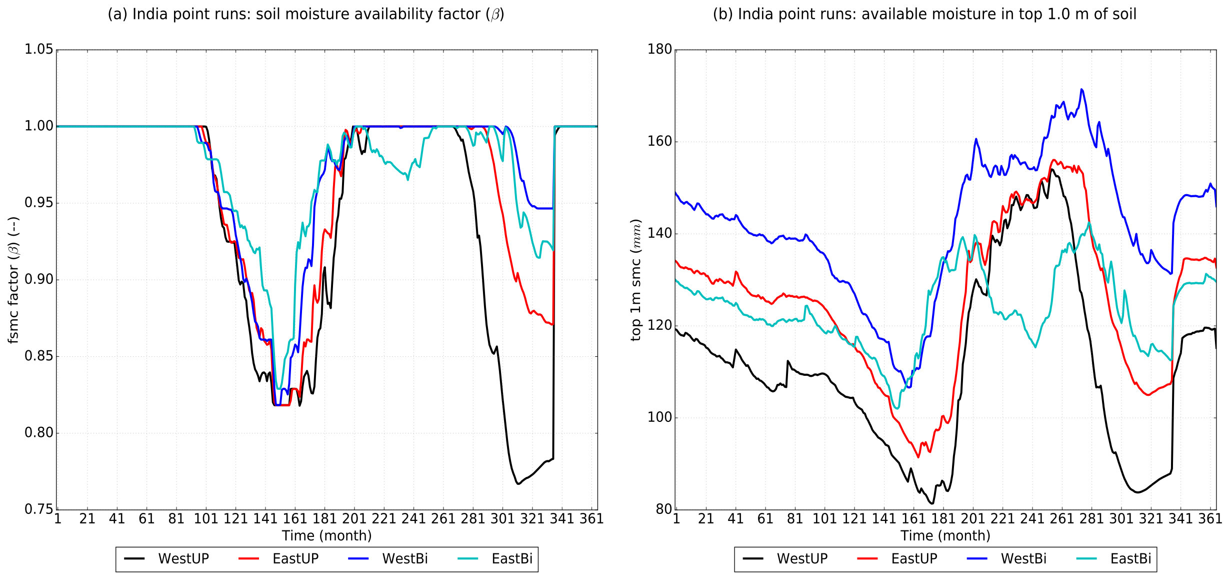

Figure 11. Annual climatology of moisture fluxes including the gridbox soil moisture availability factor (beta) (a) and the gridbox available moisture in the top 1.0 m of soil (b) at each of the India sites shown in Fig. 2. Each location is represented by a solid line of a different colour: WestUP - black, EastUP - red, WestBi - blue and EastBi - cyan

The yield observations for the region are shown in Fig. 14 for rice (a) and wheat (c); similar to the results shown for the point simulations, yields for both crops decrease from west to east. In general, the spatial distribution of rice and wheat yields are quite close to the observations, although the rice yields in JULES appear to increase slightly from west to east rather than decrease. The timeseries of the seasonal yields of rice (a, c) and wheat (b, d) area averaged for each state of Uttar Pradesh (a, b) and Bihar (c, d) are shown in Fig. 15. These show that there is considerable annual variability in the observations and the model yields. These observed yields have not been detrended, so improvements to land management practices such as irrigation or fertilization would account for increases in observed yields at the start of the timeseries. Averaging only for the Uttar Pradesh state area, the rice model yields (a) are consistently lower than observed but the wheat model yields (b) are much closer to observed until toward the end of the simulation; from 2000 to 2006 the model yields decline only recovering as the simulation finishes. However, for the Bihar state area, the rice model yields are consistently higher than the observations in all but one year (1999) and wheat yields are on a par with observations for most years in the Bihar timeseries.

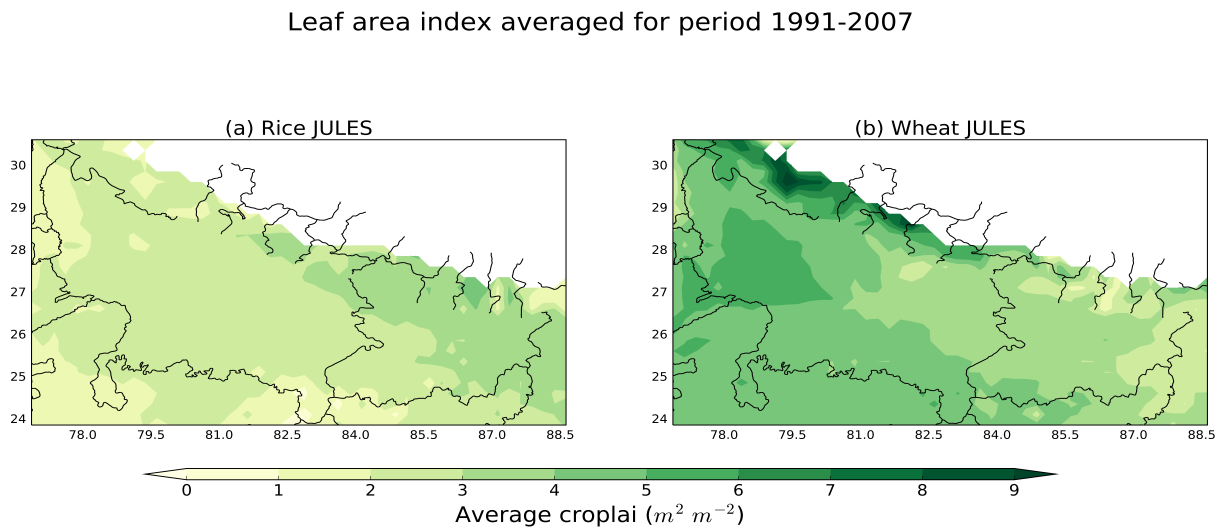

Figure 12. Average of the maximum annual crop LAI for rice and wheat for the period 1991-2007 across Uttar Pradesh and Bihar.

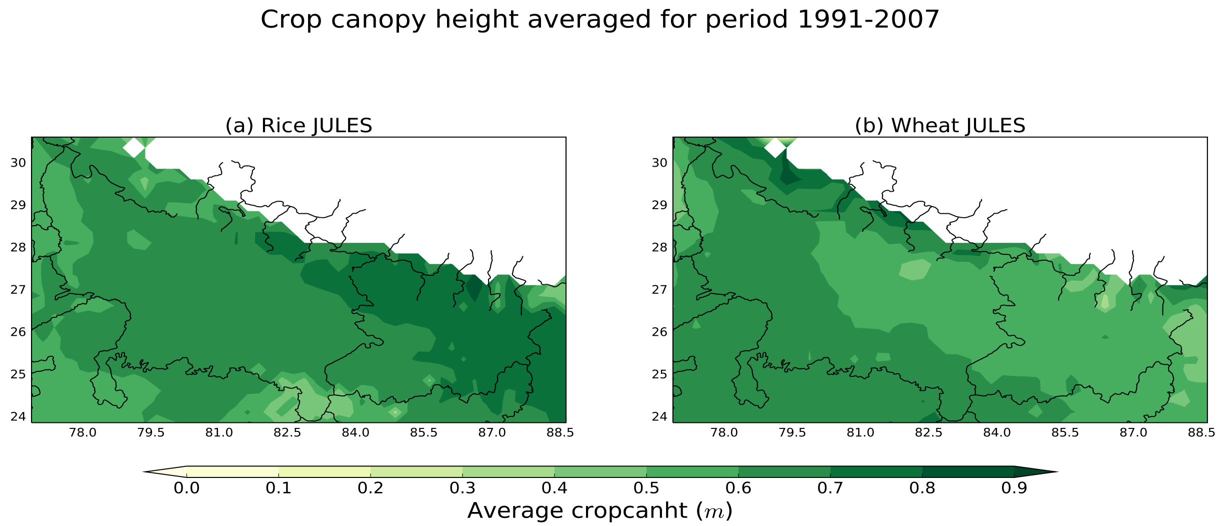

Figure 13. Average of the maximum annual crop canopy height for rice and wheat for the period 1991-2007 across Uttar Pradesh and Bihar.

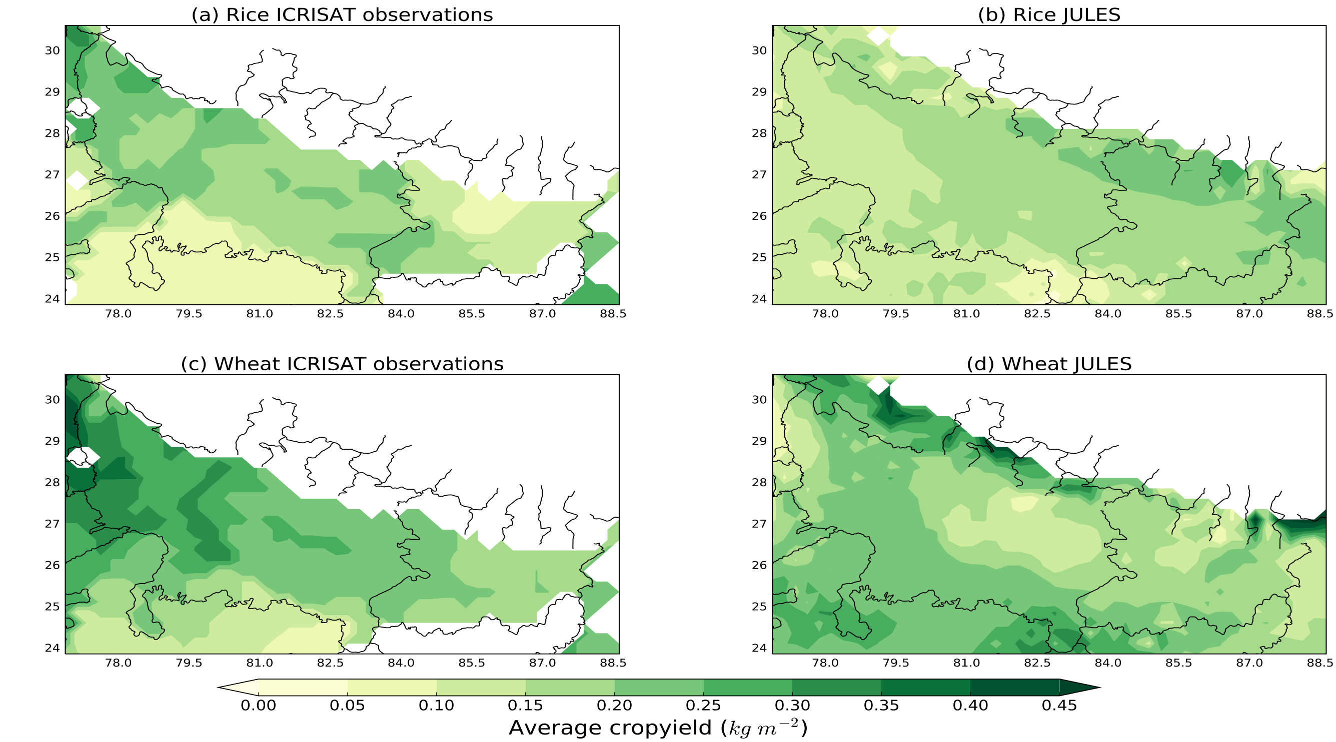

Figure 14. A comparison of observed rice yields from ICRISAT (2015) (a) with JULES rice yields (b) and observed wheat yields from ICRISAT (2015) with JULES wheat yields (d) for the period 1991-2007 across Uttar Pradesh and Bihar

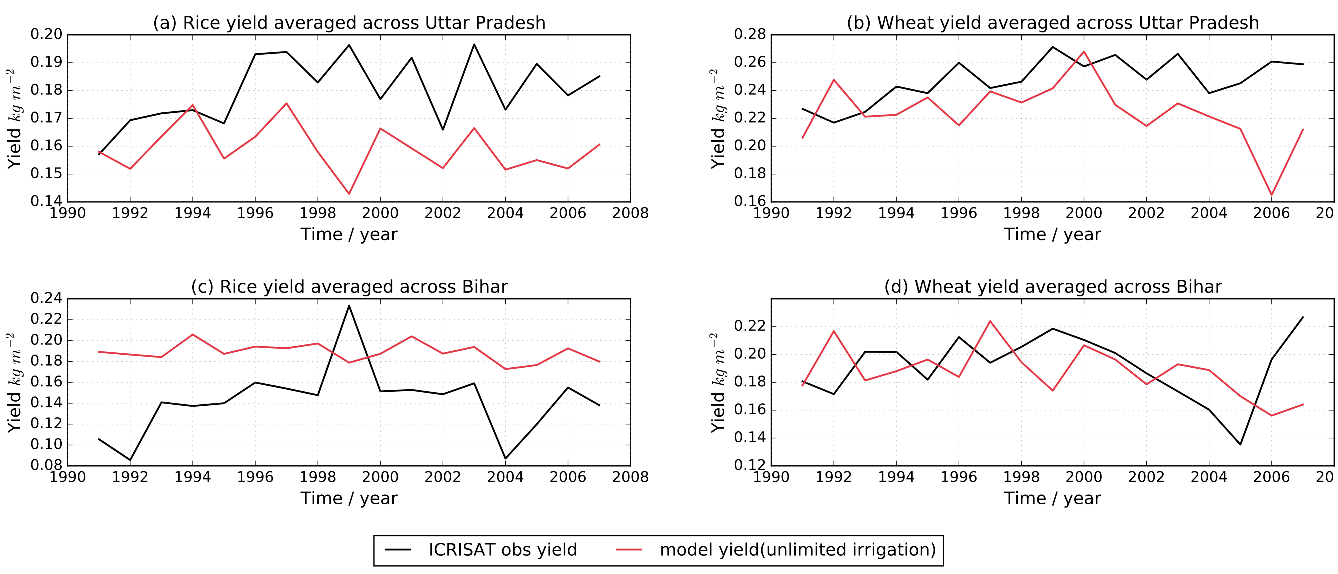

Figure 15. Annual timeseries of the yield for Uttar Pradesh and Bihar for rice and wheat.

7 Discussion

In section 6 we present point simulations for Avignon (Sect. 6.1) and both point simulations (Sect. 6.2) and a regional simulation (Sect. 6.3) for India. These simulations show that JULES is able simulate the crops sequentially, correctly reproducing the crops in rotation at the expected times of the year for several successive years. In this section we discuss these results in more detail and what they mean for future applications of the method presented.

7.1 Avignon discussion

The AviJUL simulations focus on a period between 2005 and 2013 where two crops were grown, it approximates winter wheat using spring wheat and a c4 crop based on maize to represent sorghum. During this period two varieties of sorghum were grown, with a shorter season variety grown in 2009 compared with the other two years (2007 and 2011). Although JULES does not perfectly reproduce the observations at Avignon, it does capture the different seasons and crops at this site. The 2009 sorghum is the best year in terms of model performance, with a good approximation of the LAI, canopy height and biomass. The performance of JULES compared with observations using these existing spring wheat and maize parameterizations suggests that improvements are possible by developing winter wheat and sorghum type crop parameterizations in JULES. Garrigues et al. (2015) highlight that 2006 and 2008 are two atypical years with 2006 being very dry (256 mm of rain) and 2008 being very wet (500 mm of rain); these differing conditions could explain the large differences in observed LAI and biomass between the two years (Garrigues et al., 2015).

The representation of crops either using the crop model or using grasses to represent crops has a similar effect on the surface fluxes, showing that the leaf level photosynthesis, stomatal conductance, water stress and leaf-to-canopy scaling within the model, with or without the crop model is approximated correctly. This code is used by the wider vegetation in JULES as well as the crop model.

The development of a sequential cropping capability allows the representation of the land-surface at Avignon with the observed land-cover, i.e, representing bare soil, wheat or sorghum when they are known to have been in the ground. Prior to this sequential cropping development the Avignon site would have been represented using one of two methods: The first, uses just one crop, i.e. simulating only the crop of interest. The rest of the year would most likely be represented by bare or almost bare soil. The second option is the approach used by ISIMIP (Warszawski et al., 2013, 2014); this uses a fraction of each gridbox to simulate each crop. In the first single crop option, for the season that is not of interest and therefore not being modelled explicitly the water, carbon and energy fluxes will be incorrect. For the crop that is being modelled explicitly, the initial soil moisture conditions are dependant on the previous season. The differing fluxes between the possible surface coverage options makes it difficult to know if the conditions in the single crop run at the start of each season are realistic. In the second option, two crops are modelled, thereby allowing a yield for each crop to be obtained for each gridbox; this can be postprocessed to give larger scale yields. However, it is not clear what to then use on the rest of the gridbox to produce realistic fluxes of water, energy and carbon. The results from studies that use either of these options, would not be appropriate for understanding changes in resources across a multi-crop season because there would be no coherent usage of resources between the different seasons. This means there would be no memory in the model of the conditions during the previous season and the resources used by a previous crop, which is one of the main reasons for introducing this additional complexity.

This site at Avignon is a valuable resource that will help develop and test future specific parameterizations for these crops and others that are also grown at this site. It is hoped that the suite that runs JULES at Avignon with and without sequential crops could become one of the 'golden' sites that is referred to in Williams et al. (2018) and thereby aid future development of JULES and other land surface and crop models to include a sequential cropping capability. In the following section we apply this same method to a range of locations that use the sequential cropping system in the north of India in order to implement this method for a regional tropical simulation.

7.2 India discussion

The India point and regional simulations are designed to provide similar representations of the rice–wheat crop rotation for the Uttar Pradesh and Bihar region. The observed yields for both rice and wheat are higher in the west of Uttar Pradesh and reduce as you go east across the region to Bihar. WestUP has the least available soil moisture, lowest rainfall and higher temperatures than the other locations, yet the observed yields and therefore the actual productivity are higher than for example, EastBi. The observed yields at EastBi are the lowest of the four locations, where the cooler wetter conditions should be more conducive to achieving higher yields; these are neither observed nor modelled. A combination of factors may lead to the models underestimating the WestUP wheat yields (compared to EastBi) and being much closer to observed yields in Bihar. One explanation is likely to be the differing management practices between the two states of Uttar Pradesh and Bihar. Uttar Pradesh is characterized by high agricultural productivity with effective irrigation systems (Kumar et al., 2005) and early adoption of new management practices (Erenstein and Laxmi, 2008). Bihar on the other hand has lower agricultural productivity, farms tend to be smaller and more fragmented, irrigation systems are less effective (Laik et al., 2014) and adoption of new technology is also slower due to the lack of available machinery (Erenstein and Laxmi, 2008). Yield gap parameters are included in many crop models in order to account for the impact of differing nutrient levels, pests, diseases and non-optimal management (Challinor et al., 2004), thus explaining the difference between potential and actual yield under the same environment Fischer (2015). This is not included in these simulations.

An alternative explanation for the difference in model yields from west to east could also be that at the western locations, the humidity is lower (higher VPD) and the temperatures are higher; these conditions may provide another contributory factor for the model underestimating the yields there. The humidity in the simulations could be lower in these simulations than in reality for two reasons: first we are running JULES in standalone mode. This means that the land-surface and therefore the crop is unable to influence the atmosphere through evaporation because the humidity is prescribed by the driving data at each timestep. Second the driving data is from an RCM that does not include irrigation (Mathison et al., 2015) so the humidity in the driving data is not modified by evaporation due to irrigation. We are therefore missing the part of the water cycle that allows evaporation from the surface to affect the humidity. This region is intensively irrigated (Biemans et al., 2013) which means that there is a significant contribution from the evaporation due to irrigation and the recycling of water into precipitation (Harding et al., 2013; Tuinenburg et al., 2014) that cannot be accounted for here. Tuinenburg et al. (2014) estimate that as much as 35

% of the evaporation moisture from the Ganges basin is recycling within the river basin. We hypothesize that the VPD may be too high in our forcing data and this could be affecting the model yields at this location (Ocheltree et al., 2014).

The yields in the model are also affected by the other choices made in setting up the model. For example, the stage at which leaf senescence begins is given by a user defined parameter in JULES (sen_dvi_io). In these simulations this is set to be when the DVI is equal to 1.5. At this stage the carbon from the leaves starts to be remobilized to the harvest pool (Fig. 9); which consists of both the reproductive parts of the plants and the yellow leaves (Williams et al., 2017). During this senescence period, the plants continue to respire but as the leaves are lost photosynthesis reduces. This results in a decline in NPP, which begins too early in the season. In addition the allometric coefficients that control the partitioning of carbon to the different parts of the crop in JULES are currently those from Osborne et al. (2015); it is possible that the results could be improved for South Asia if these were tuned to more appropriate values for the crops there.

In these India simulations (both point and regional) we assume that irrigation only occurs during the wheat season with no irrigation during the rice season, because rice is grown during the wettest part of the year. Some irrigation may occur during monsoon breaks. It would be useful to develop JULES to recognise a break in monsoon rainfall and trigger irrigation of rice if the monsoon break is accompanied by a drop-in soil moisture. Also, temperatures in JULES cannot damage any of the crops being modelled either by being too high, too low or not low enough. Future work using JULES-crop would benefit from developments to enable the model to simulate when and where crops suffer from heat stress or problems with soil nutrients, pests and diseases and for these to be able to have an impact on crop yields.

The simulations shown here consider a small number of rotations, crops and regions. However; different varieties and types of crops; the timings of sowing and harvesting; together with many possible irrigation options can have a large impact on the model results. This is an important consideration for future work and should be investigated fully when applying this method to new areas.

8 Conclusions

In this paper we describe and demonstrate a new development for JULES enabling more than one crop to be simulated at a given location during a particular growing season, thereby including a sequential cropping capability. This is an important development, allowing more accurate representation of land use and surface coverage in regions where two or more crops are grown in rotation. Including the correct land-use and surface coverage in models means that the simulations can produce more realistic fluxes of carbon, water and energy; these are important for understanding the impacts of climate change. The continuous simulation of all crops throughout the year also provides a more complete picture of the total demand for water resources which is important for climate impacts assessments. There are relatively few models that are able to simulate sequential cropping, but there is a growing need as more regions of the world adopt this cropping system as a viable way of adapting to climate change (Hudson, 2009). We demonstrate the method and evaluate its impact for a site in Avignon; this a site that has grown crops in rotation for several years and therefore has a lengthy and detailed observation record. We use this site to simulate a winter wheat–sorghum rotation in JULES approximated using spring wheat and maize. We apply this same method to four locations that use the sequential cropping system in the northern Indian states of Uttar Pradesh and Bihar, in order to inform its implementation for a regional simulation of South Asia.

We show that JULES is able to simulate two crops in a year both at Avignon and across Uttar Pradesh and Bihar, producing maxima of LAI, canopy height and biomass at approximately the correct times of the year. The wealth of observations at Avignon also provide the opportunity to gain a better understanding of the effect of sequential cropping on the surface fluxes. JULES is successful in producing two realistic crops at Avignon, with crops changing from one to another in a single growing period and generally reproducing the observed surface fluxes; the GPP and energy fluxes (H and LE) correlate well with observations with r values of above 0.7. However the magnitude of the biomass for wheat is underestimated and LAI is overestimated compared with Avignon observations. In the simulations where grasses are used to represent the crops at Avignon the fluxes also correlate well with the observations (r values greater than 0.7), this shows that the parts of JULES that are shared with JULES-crop are performing well at Avignon. In general there are only small differences between using the crop model and using grasses to represent the crops at this site, indicating that JULES-crop can reproduce the LAI and canopy height well enough to compare well with the observed surface fluxes. There are two varieties of sorghum grown at this site and this is apparent from the differences in the JULES simulations presented. Using maize as an approximation for sorghum provides a better representation for the variety grown in 2009 than in either of the 2007 or 2011 seasons. The representation of crops at Avignon could be improved by including crop specific parameterizations of winter wheat and sorghum in the model, although sorghum would probably require two different sets of parameters for a significant improvement because the two varieties grown at the site are so different.

The sequential cropping system is used widely in the Tropics, especially regions such as Pakistan, India and Bangladesh. We run a regional simulation of JULES for the Indian states of Uttar Pradesh and Bihar and also for four locations within these states; these are two of the main producers of rice and wheat in India and use of the rice–spring wheat rotation is prevalent in this region. This region is highly variable, both in terms of temperatures (ranging from 7 to 52 $^\circ$ C) and rainfall (between 0 and 15 $\mathrm{mm\ day^{-1}}$) with these locations showing a cooling moistening trend from west to east making conditions for growing crops very different across a relatively limited area. JULES produces both a rice and wheat crop across the region and for each of the four location simulations, with yields for the locations in the cooler, wetter east of the region closer to observed yields than those in the warmer drier west. We propose two possible reasons for this difference, although in reality both could be contributing factors. One explanation for the differences in observed yields between WestUP and EastBi is the differing management practices between the two states of Uttar Pradesh and Bihar. The western locations are typically more effective at adopting new technology and therefore have higher yields than the eastern locations. This difference from west to east may therefore be reduced by a yield gap parameter. Alternatively ensuring that irrigation is represented in the forcing climate data used to drive JULES may reduce the differences between the observed and model yields at WestUP. The lack of irrigation in the forcing data, could reduce evaporation from the surface. Tuinenburg et al. (2014) highlight that this makes a considerable contribution to the overall moisture budget for South Asia.

The work presented here has shown that sequential cropping is an important addition to JULES, providing a closer representation of the land surface where crops are grown in rotation. Therefore the code modifications presented as part of this analysis, currently in a branch of JULES at vn5.2, are intended for inclusion in a future official version of JULES. This analysis has provided valuable information for using this sequential cropping method for future larger crop simulations. Model intercomparison projects such as AgMIP (Rivington and Koo, 2010; Rosenzweig et al., 2013, 2014) and ISIMIP (Warszawski et al., 2013, 2014) have hugely benefited the crop and land-surface modelling communities by accelerating development and understanding of land surface models. On the basis that this cropping system is likely to be a feature of the future land-surface, not just in the tropics but globally as an adaptation to climate change, we encourage other modelling communities to develop their models to include a sequential cropping capability so that future model intercomparisons can include this and find ways to improve it further.

Code and data availability. The JULES model code used in this paper is available from the Met Office Science Repository Service on registering: https://code.metoffice.gov.uk/trac.
The version of the model used in this analysis is an enhanced JULESvn5.2, this branch is available from this link:
https://code.metoffice.gov.uk/trac/jules/browser/main/branches/dev/camillamathison/vn5.2_croprotate_irrigtiles.
The developments contained in this branch will hopefully be implemented into the trunk of JULES in the near future. The regional climate model datasets used will hopefully be available via the Centre for Environmental Data Analysis (CEDA) catalogue. It is hoped that the Avignon rose suite will also be made available in order to aid future model development.

9 Appendix A: Avignon comparison

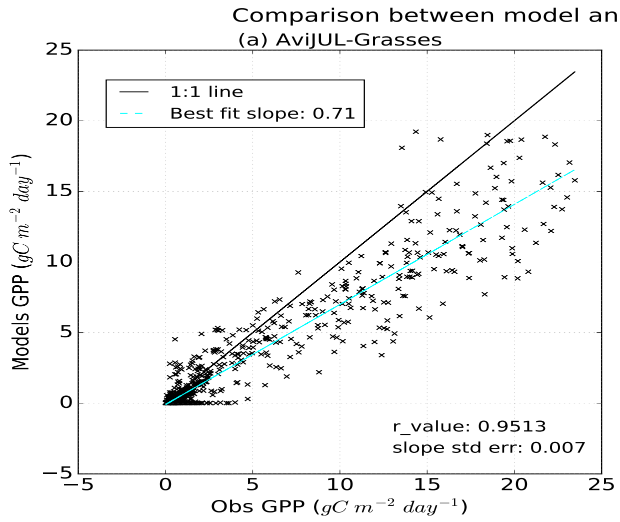

Figure A.1. Comparison of Observed GPP at the Avignon site against the modelled GPP between 2005 and 2008 for AviJUL-grass (a) and AviJUL-sqcrop (b)

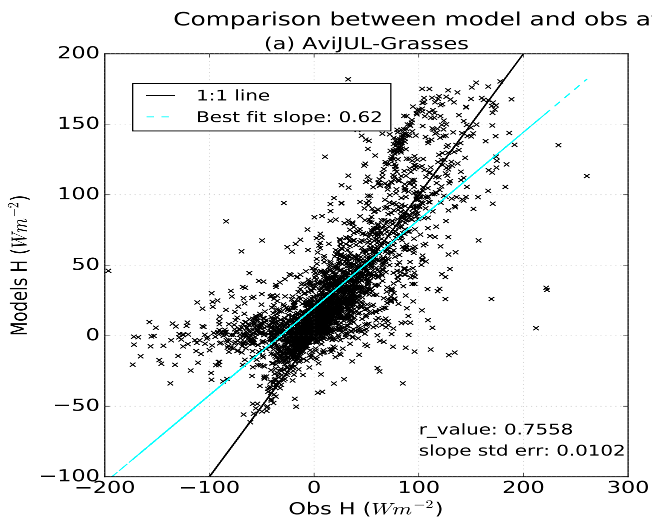

Figure A.2. Comparison of observed H at the Avignon site against the modelled H between 2005 and 2013 for AviJUL-grass (a) and AviJUL-sqcrop (b)

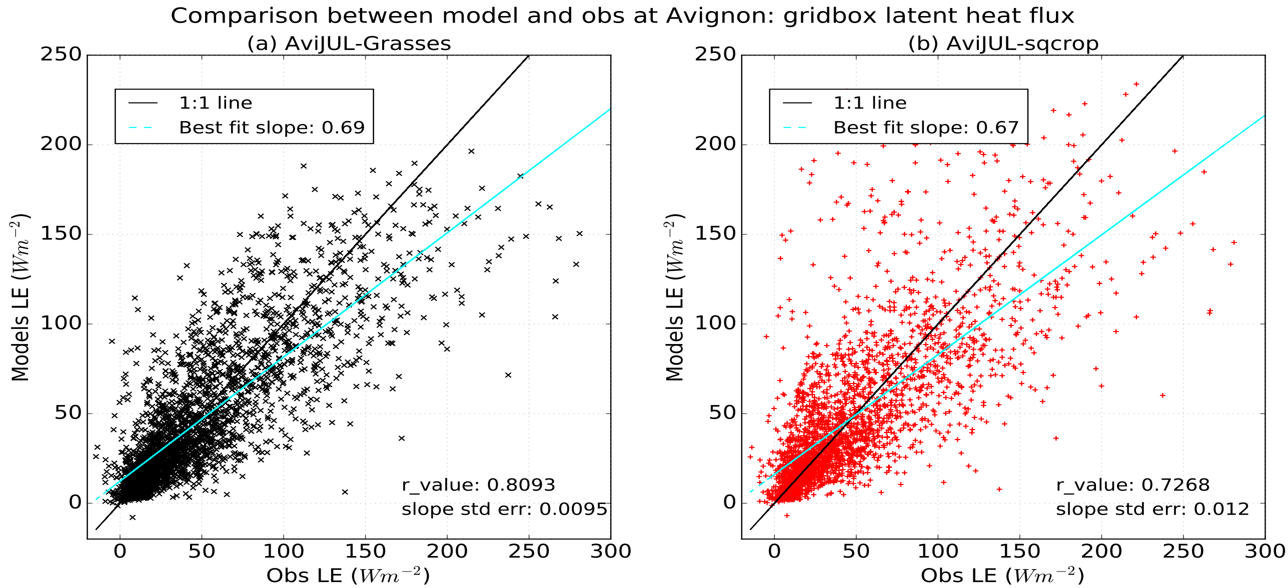

Figure A.3. Comparison of observed LE at the Avignon site against the modelled LE between 2005 and 2013 for AviJUL-grass (a) and AviJUL-sqcrop (b).

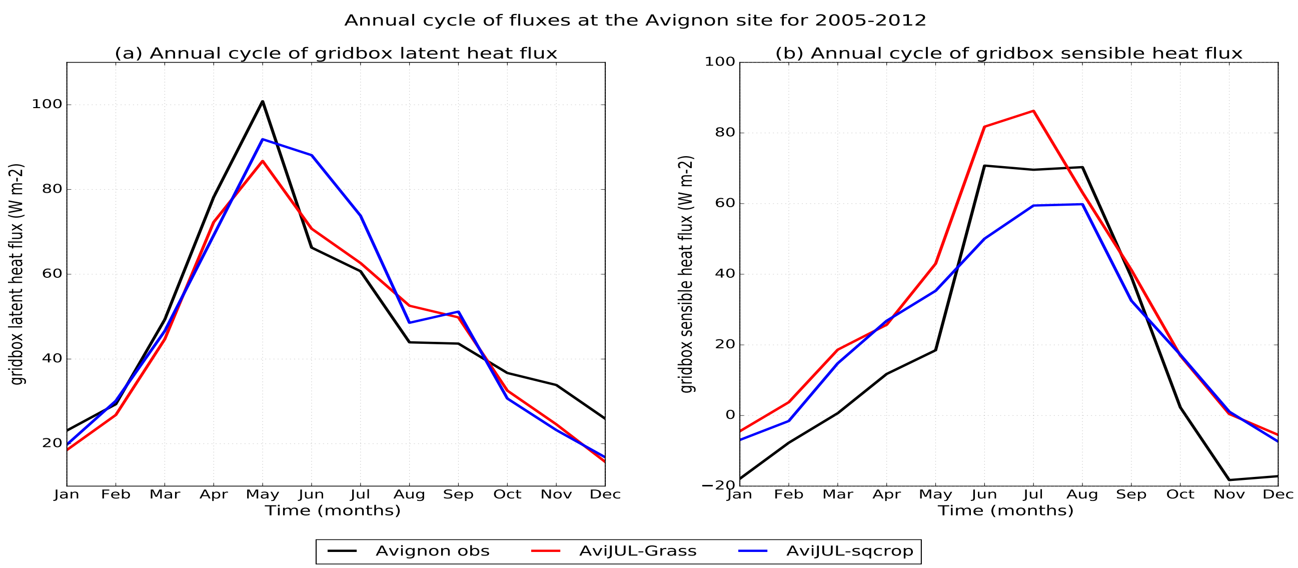

Figure A.4. Annual cycle of the H and LE compared with observations (black line) at the Avignon site for between 2005 and 2013. Annual cycles for the simulations are also shown: AviJUL-grass (red line). AviJUL-sqcrop (blue line).

10 Appendix B: India point comparison

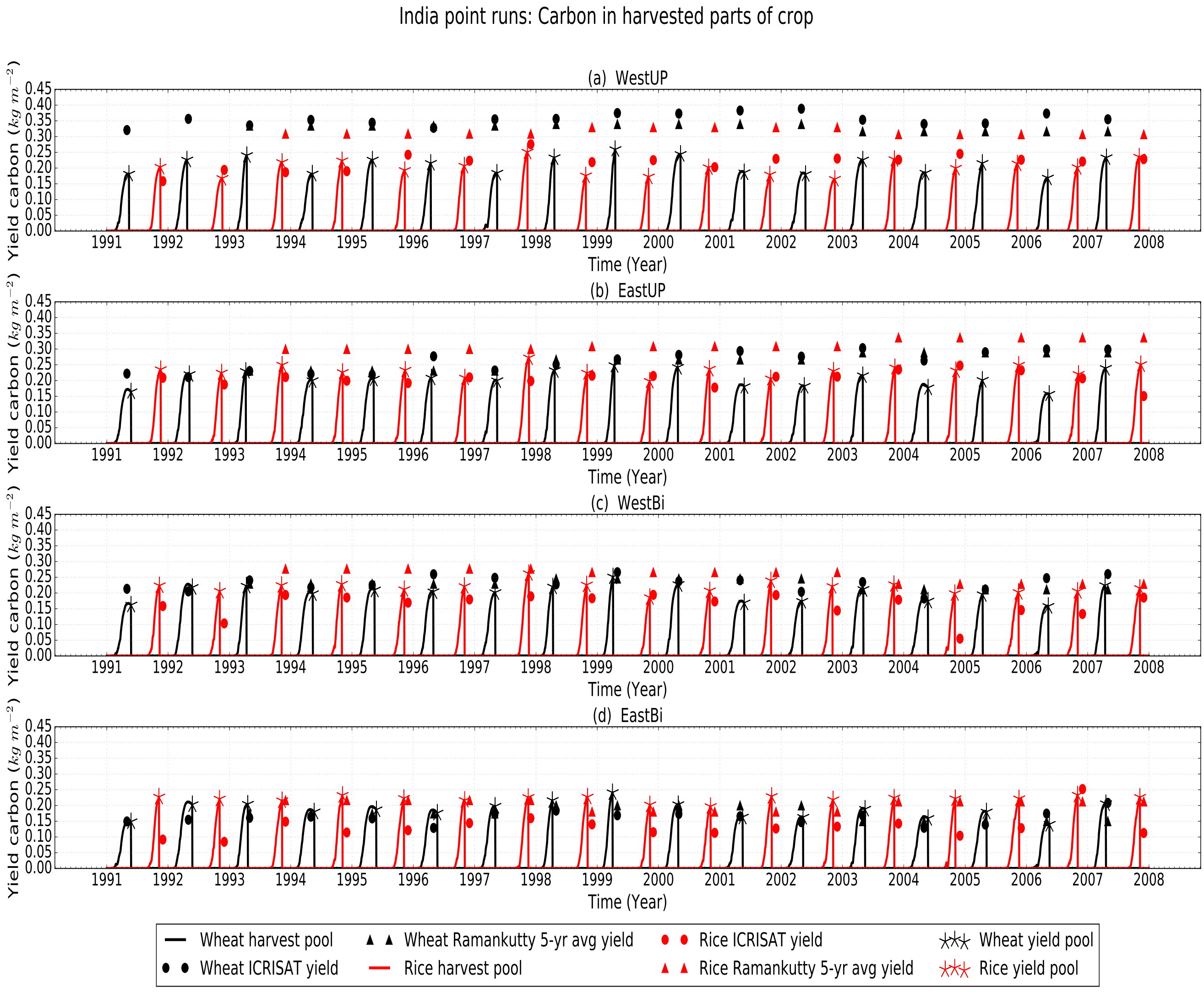

Figure B.1. Timeseries of crop harvest pool (solid lines) with the JULES yield at the time it is output by the model (asterisks) for rice (red) and wheat (black) at each of the India sites shown in Fig. 2. Also shown are two sets of observations; annual yields from ICRISAT (2015) shown by the filled circles and 5 year averages from Ray et al. (2012a) shown by the filled triangles (following the same colours with rice shown in red and wheat in black)

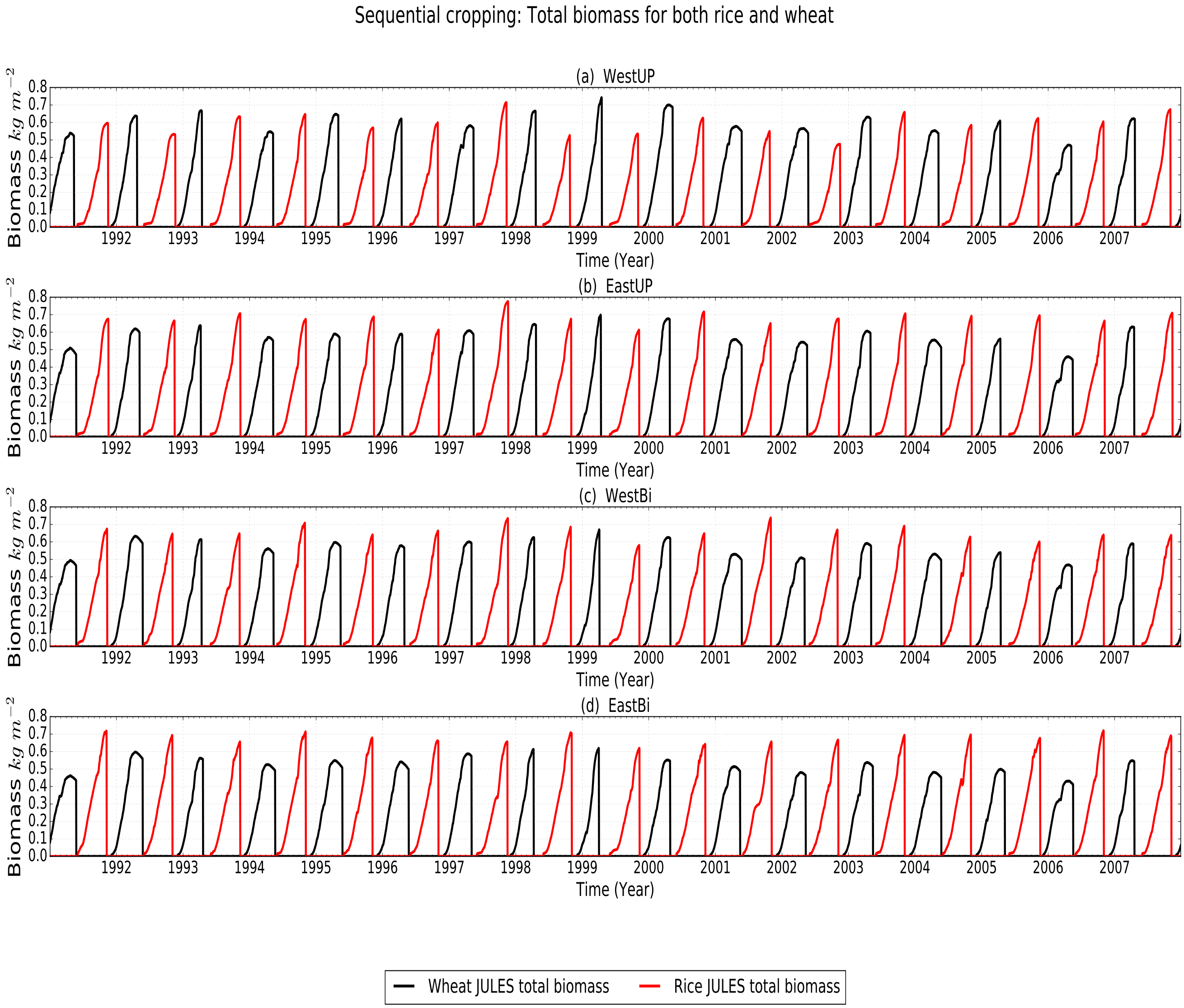

Figure B.2. Timeseries of total biomass for rice (red) and wheat (black) at each of the India sites shown in Fig. 2.

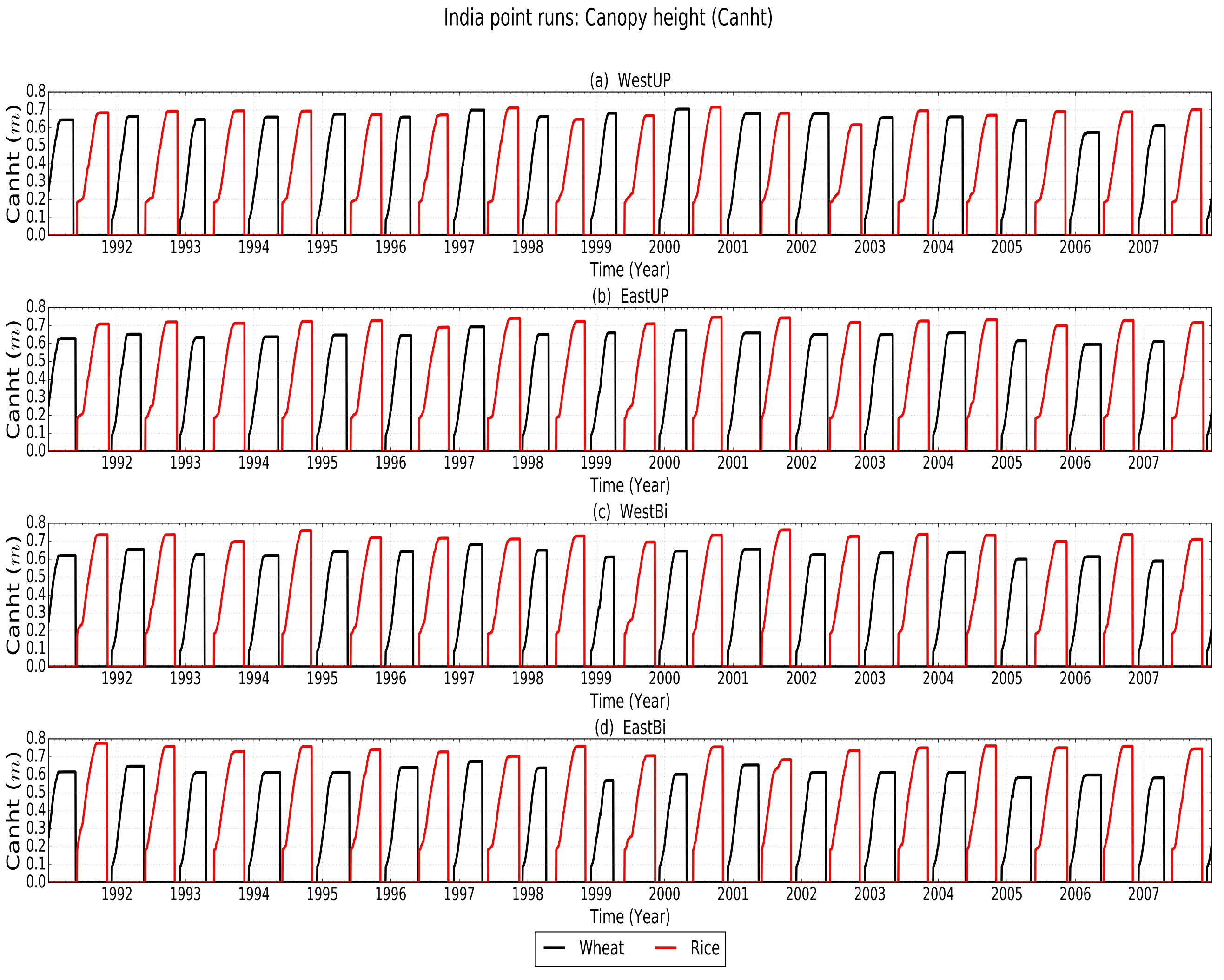

Figure B.3. Timeseries of canopy height for rice (red) and wheat (black) at each of the India sites shown in Fig. 2.

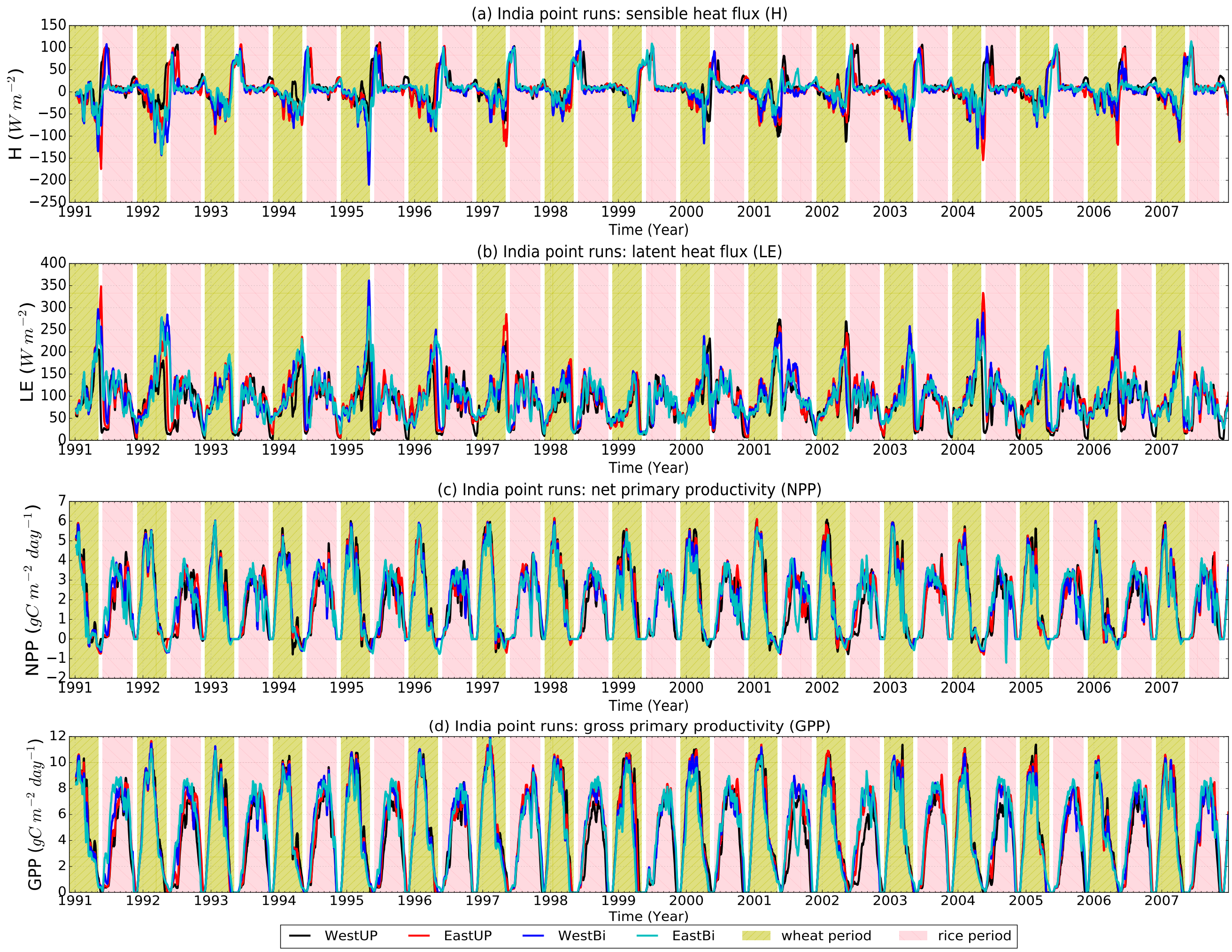

Figure B.4. Timeseries of LE (a), H (b), gridbox NPP (c) and gridbox GPP (d) at each of the India sites shown in Fig. 2. Each location is represented by a solid line of a different colour: WestUP - black, EastUP - red, WestBi - blue and EastBi - cyan

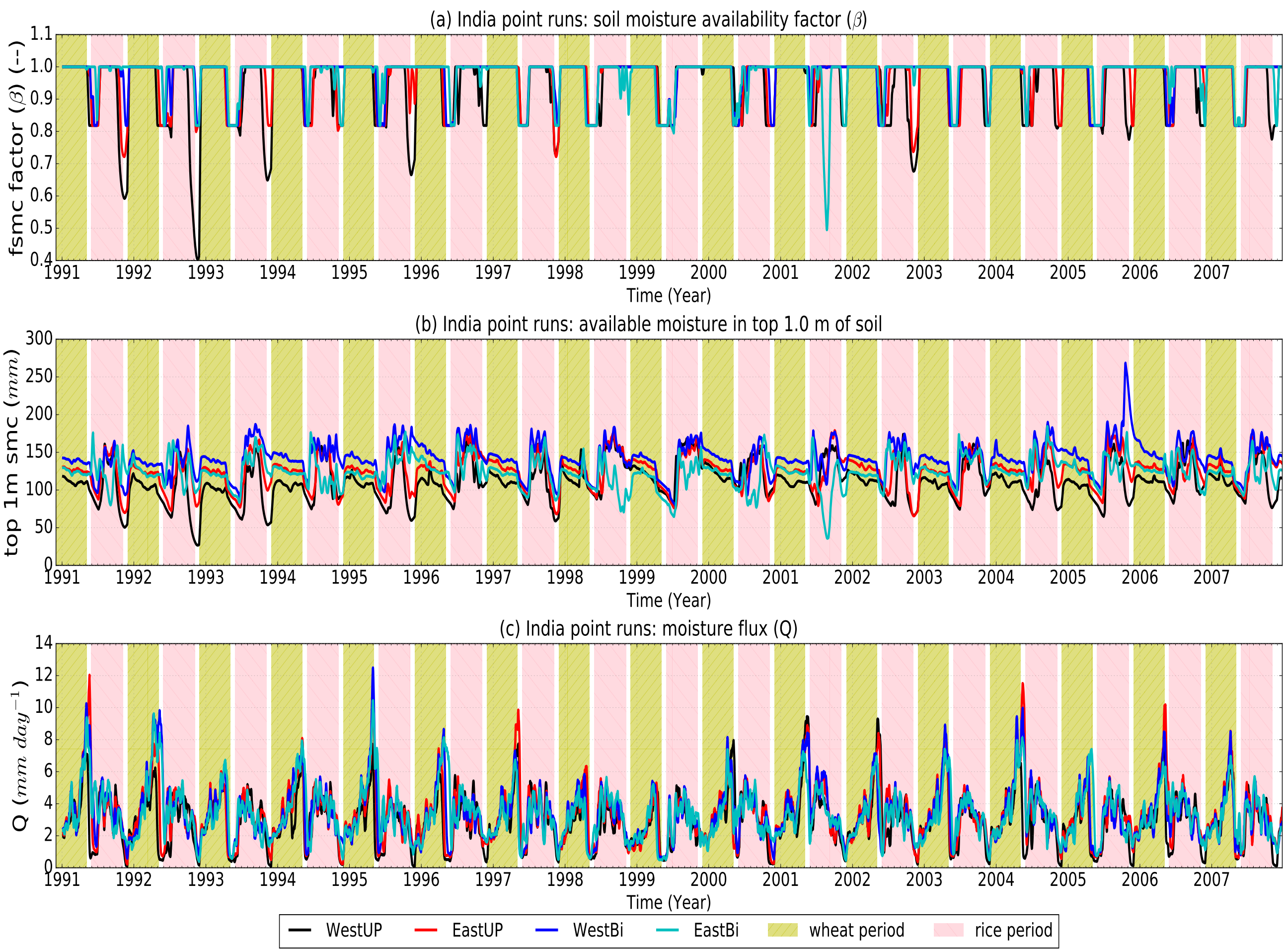

Figure B.5. Timeseries of moisture fluxes including the gridbox soil moisture availability factor (beta) (a), the gridbox available moisture in the top 1.0 m of soil (b) and moisture flux across the gridbox (c) at each of the India sites shown in Fig. 2. Each location is represented by a solid line of a different colour: WestUP - black, EastUP - red, WestBi - blue and EastBi - cyan

11 Appendix C: India regional simulation

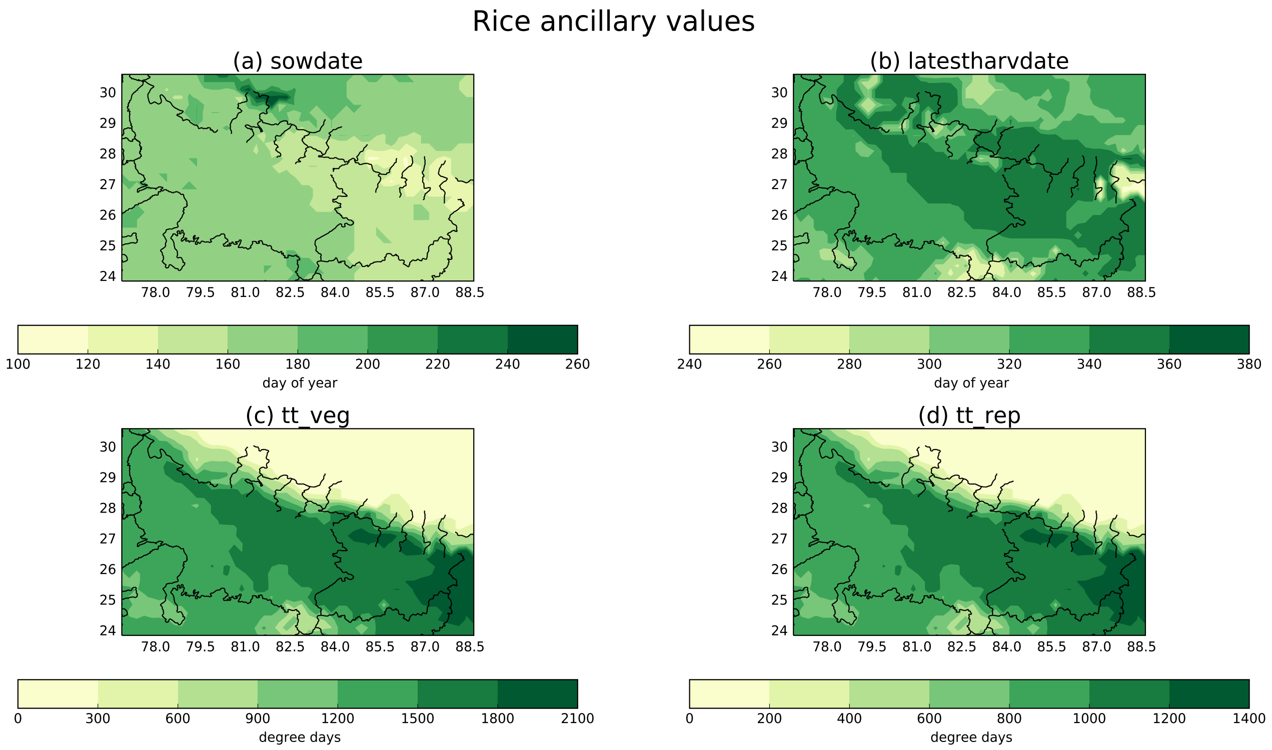

Figure C.1. The values used in the regional JULES ancillary for rice. Sowing date (a) and latest possible harvest date (b), both in units of day of year. Thermal time for the vegetative stage (c) and thermal time for the reproductive stage (d) both in units of degree days

.

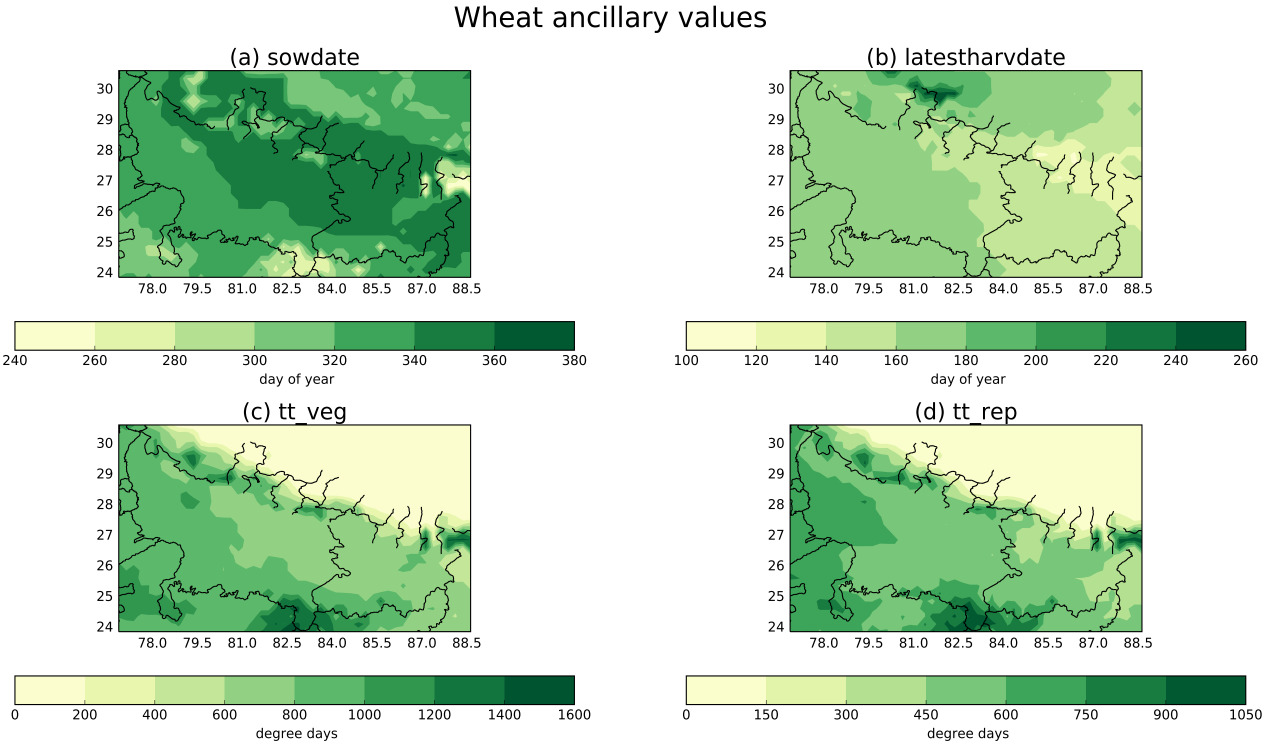

Figure C.2. The values used in the regional JULES ancillary for wheat. Sowing date (a) and latest possible harvest date (b), both in units of day of year. Thermal time for the vegetative stage (c) and thermal time for the reproductive stage (d) both in units of degree days

.

Author contributions. Andrew J Challinor, Pete Falloon and Andy Wiltshire provided general scientific guidance throughout the paper and helped prioritise the initial requirement for including sequential cropping in JULES, toward the aim of modelling integrated impacts for South Asia. Chetan Deva provided gridded observations of cropyield courtesy of ICRISAT. Sébastien Garrigues and Sophie Moulin provided Avignon data. Karina Williams provided code for generating the crop ancillary files and an initial suite for Avignon without crops.

Competing interests. The authors declare that they have no conflict of interest.

Acknowledgements. The research leading to these results has received funding from the European Union Seventh Framework Programme FP7/2007–2013 under grant agreement no. 603864. Camilla Mathison, Pete Falloon, Andy Wiltshire and Karina Williams were supported by the Met Office Hadley Centre Climate Programme funded by BEIS and Defra. Thanks also to Kate Halladay for helping me understand the soil moisture and irrigation implications. The authors thank the INRA EMMAH laboratory at Avignon (France) in charge of the "flux and remote sensing site" for the supply of the data.

References

Allen, R. G., Pereira, L. S., Raes, D., and Smith, M.: Crop evapotranspiration - Guidelines for computing crop water requirements - FAO Irrigation and drainage paper 56, Food and Agriculture Organization of the United Nations, www.fao.org/3/X0490E/x0490e00.htm, 1998.

Best, M. J., Pryor, M., Clark, D. B., Rooney, G. G., Essery, R. L. H., Ménard, C. B., Edwards, J. M., Hendry, M. A., Porson, A., Gedney, N., Mercado, L. M., Sitch, S., Blyth, E., Boucher, O., Cox, P. M., Grimmond, C. S. B., and Harding, R. J.: The Joint UK Land Environment Simulator (JULES), model description, Part 1: Energy and water fluxes, Geoscientific Model Development, 4, 677–699, https://doi.org/10.5194/gmd-4-677-2011, http://www.geosci-model-dev.net/4/677/2011/, 2011.

Betts, R. A.: Integrated approaches to climate-crop modelling: needs and challenges, Philosophical transactions of the Royal Society of London. Series B, Biological sciences, 360, 2049–65, https://doi.org/10.1098/rstb.2005.1739, 2005.

Bhattacharyya, T., Pal, D., Easter, M., Batjes, N., Milne, E., Gajbhiye, K., Chandran, P., Ray, S., Mandal, C., Paustian, K., Williams, S., Killian, K., Coleman, K., Falloon, P., and Powlson, D.: Modelled soil organic carbon stocks and changes in the Indo-Gangetic Plains, India from 1980 to 2030, Agriculture, Ecosystems & Environment, 122, 84 – 94, https://doi.org/https://doi.org/10.1016/j.agee.2007.01.010, http://www.sciencedirect.com/science/article/pii/S0167880907000394, soil carbon stocks at regional scales, 2007.

Biemans, H., Speelman, L., Ludwig, F., Moors, E., Wiltshire, A., Kumar, P., Gerten, D., and Kabat, P.: Future water resources for food production in five South Asian river basins and potential for adaptation - A modeling study, Science of The Total Environment, 468-469, Supplement, S117–S131, https://doi.org/http://dx.doi.org/10.1016/j.scitotenv.2013.05.092, http://dx.doi.org/10.1016/j.scitotenv.2013.05.092, 2013.

Biemans, H., Siderius, C., Mishra, A., and Ahmad, B.: Crop-specific seasonal estimates of irrigation-water demand in South Asia, Hydrology and Earth System Sciences, 20, 1971–1982, https://doi.org/10.5194/hess-20-1971-2016, 2016.

Bodh, S. P. C., Rai, S. J. P., Sharma, S. A., Gajria, S. P., Yadav, S. M., Virmani, S. S., and Pandey, S. R.: Agricultural Statistics at a Glance 2015, Ministry of Agriculture & Farmers welfare, Directorate of Economics and Statistics, http://eands.dacnet.nic.in, 2015.

Bondeau, A., Smith, P. C., Zaehle, S., Schaphoff, S., Lucht, W., Cramer, W., Gerten, D., Lotze-Campen, H., Müller, C., Reichstein, M., and Smith, B.: Modelling the role of agriculture for the 20th century global terrestrial carbon balance, Global Change Biology, 13, 679–706, https://doi.org/10.1111/j.1365-2486.2006.01305.x, https://onlinelibrary.wiley.com/doi/abs/10.1111/j.1365-2486.2006.01305.x, 2007.

Caldwell, R. M. and Hansen, J. W.: Simulation of multiple cropping systems with CropSys, pp. 397–412, Springer Netherlands, Dordrecht, https://doi.org/10.1007/978-94-011-2842-1_24, https://doi.org/10.1007/978-94-011-2842-1_24, 1993.

Calvet, J.-C., Noilhan, J., Roujean, J.-L., Bessemoulin, P., Cabelguenne, M., Olioso, A., and Wigneron, J.-P.: An interactive vegetation SVAT model tested against data from six contrasting sites, Agricultural and Forest Meteorology, 92, 73–95, https://doi.org/10.1016/S0168-1923(98)00091-4, 1998.

Challinor, A., Wheeler, T., Craufurd, P., Slingo, J., and Grimes, D.: Design and optimisation of a large-area process-based model for annual crops, Agricultural and Forest Meteorology, 124, 99 – 120, https://doi.org/https://doi.org/10.1016/j.agrformet.2004.01.002, http://www.sciencedirect.com/science/article/pii/S0168192304000085, 2004.

Clark, D. B., Mercado, L. M., Sitch, S., Jones, C. D., Gedney, N., Best, M. J., Pryor, M., Rooney, G. G., Essery, R. L. H., Blyth, E., Boucher, O., Harding, R. J., Huntingford, C., and Cox, P. M.: The Joint UK Land Environment Simulator (JULES), model description, Part 2: Carbon fluxes and vegetation dynamics, Geoscientific Model Development, 4, 701–722, https://doi.org/10.5194/gmd-4-701-2011, http://www.geosci-model-dev.net/4/701/2011/, 2011.

Cong, W.-F., Hoffland, E., Li, L., Six, J., Sun, J.-H., Bao, X.-G., Zhang, F.-S., and Werf, W. V. D.: Intercropping enhances soil carbon and nitrogen, Global Change Biology, 21, 1715–1726, https://doi.org/10.1111/gcb.12738, https://onlinelibrary.wiley.com/doi/abs/10.1111/gcb.12738, 2015.

Dee, D. P., Uppala, S. M., Simmons, A. J., Berrisford, P., Poli, P., Kobayashi, S., Andrae, U., Balmaseda, M. A., P., G. B., Bauer, Bechtold, P., Beljaars, A. C. M., van de Berg, L., Bidlot, J., Bormann, N., Delsol, C., Dragani, R., Fuentes, M., Geer, A. J., Haimberger, L., Healy, S. B., Hersbach, H., Hólm, E. V., Isaksen, L., Kållberg, P., Köhler, M., Matricardi, M., McNally, A. P., Monge-Sanz, B. M., Morcrette, J.-J., Park, B.-K., Peubey, C., de Rosnay, P., Tavolato, C., Thépaut, J.-N., and Vitart, F.: The ERA-Interim reanalysis: configuration and performance of the data assimilation system, Quarterly Journal of the Royal Meteorological Society, 137, 553–597, https://doi.org/10.1002/qj.828, http://dx.doi.org/10.1002/qj.828, 2011.

Dury, J., Schaller, N., Garcia, F., Reynaud, A., and Bergez, J. E.: Models to support cropping plan and crop rotation decisions. A review, Agronomy for Sustainable Development, 32, 567–580, https://doi.org/10.1007/s13593-011-0037-x, https://doi.org/10.1007/s13593-011-0037-x, 2012.

Erenstein, O. and Laxmi, V.: Zero tillage impacts in India's rice-wheat systems: A review, Soil and Tillage Research, 100, 1 – 14, https://doi.org/https://doi.org/10.1016/j.still.2008.05.001, http://www.sciencedirect.com/science/article/pii/S0167198708000822, 2008.

Erenstein, O., Farooq, U., Malik, R., and Sharif, M.: On-farm impacts of zero tillage wheat in South Asia's rice-wheat systems, Field Crops Research, 105, 240–252, https://doi.org/https://doi.org/10.1016/j.fcr.2007.10.010, http://www.sciencedirect.com/science/article/pii/S0378429007002067, 2008.

Essery, R. L. H., Best, M. J., and Cox, P. M.: MOSES 2.2 technical documentation, Hadley Centre Technical Note, 30, http://www.metoffice.gov.uk/archive/hadley-centre-technical-note-30, 2001.

Fischer, R.: Definitions and determination of crop yield, yield gaps, and of rates of change, Field Crops Research, 182, 9–18, https://doi.org/10.1016/j.fcr.2014.12.006, 2015.

Frieler, K., Levermann, A., Elliott, J., Heinke, J., Arneth, A., Bierkens, M. F. P., Ciais, P., Clark, D. B., Deryng, D., Döll, P., Falloon, P., Fekete, B., Folberth, C., Friend, A. D., Gellhorn, C., Gosling, S. N., Haddeland, I., Khabarov, N., Lomas, M., Masaki, Y., Nishina, K., Neumann, K., Oki, T., Pavlick, R., C.Ruane, A., Schmid, E., Schmitz, C., Stacke, T., Stehfest, E., Tang, Q., Wisser, D., Huber, V., Piontek, F., Warszawski, L., Schewe, J., Lotze-Campen, H., and Schellnhuber, H. J.: A framework for the cross-sectoral integration of multi-model impact projections: land use decisions under climate impacts uncertainties, Earth System Dynamics, 6, 447–460, https://doi.org/10.5194/esd-6-447-2015, https://www.earth-syst-dynam.net/6/447/2015/, 2015.

Garrigues, S., Olioso, A., Calvet, J., Martin, E., Lafont, S., Moulin, S., Chanzy, A., Marloie, O., Buis, S., Desfonds, V., Bertrand, N., and Renard, D.: Evaluation of land surface model simulations of evapotranspiration over a 12-year crop succession: impact of soil hydraulic and vegetation properties, Hydrology and Earth System Sciences, 19, 3109–3131, https://doi.org/10.5194/hess-19-3109-2015, https://www.hydrol-earth-syst-sci.net/19/3109/2015/, 2015.

Garrigues, S., Boone, A., Decharme, B., Olioso, A., Albergel, C., Calvet, J.-C., Moulin, S., Buis, S., and Martin, E.: Impacts of the Soil Water Transfer Parameterization on the Simulation of Evapotranspiration over a 14-Year Mediterranean Crop Succession, Journal of Hydrometeorology, 19, 3–25, https://doi.org/10.1175/JHM-D-17-0058.1, https://doi.org/10.1175/JHM-D-17-0058.1, 2018.

Goswami, B. and Xavier, P. K.: Dynamics of "internal" interannual variability of the Indian summer monsoon in a GCM, Journal of Geophysical Research: Atmospheres, 110, n/a–n/a, https://doi.org/10.1029/2005JD006042, http://dx.doi.org/10.1029/2005JD006042, 2005.

Griffiths, F. E. W., Lyndon, R., and Bennett, M.: The Effects of Vernalization on the Growth of the Wheat Shoot Apex, Annals of Botany, 56, 501–511, https://doi.org/10.1093/oxfordjournals.aob.a087035, 1985.

Harding, R., Blyth, E., Tuinenburg, O., and Wiltshire, A.: Land atmosphere feedbacks and their role in the water resources of the Ganges basin, Science of The Total Environment, 468-469, Supplement, S85 – S92, https://doi.org/http://dx.doi.org/10.1016/j.scitotenv.2013.03.016, http://www.sciencedirect.com/science/article/pii/S0048969713003070, changing water resources availability in Northern India with respect to Himalayan glacier retreat and changing monsoon patterns: consequences and adaptation, 2013.

Harper, A. B., Williams, K., Team, J., and Team, F.: Toward an improved representation of soil moisture stress: disentangling causes and effects, to be decided, 00, 0–34, in preparation.

Hatfield, J. L. and Prueger, J. H.: Temperature extremes: Effect on plant growth and development, Weather and Climate Extremes, 10, 4 – 10, https://doi.org/https://doi.org/10.1016/j.wace.2015.08.001, http://www.sciencedirect.com/science/article/pii/S2212094715300116, uSDA Research and Programs on Extreme Events, 2015.

Hu, S., Mo, X., and Lin, Z.: Optimizing the photosynthetic parameter Vcmax by assimilating MODIS-fPAR and MODIS-NDVI with a process-based ecosystem model, Agricultural and Forest Meteorology, 198-199, 320 – 334, https://doi.org/https://doi.org/10.1016/j.agrformet.2014.09.002, http://www.sciencedirect.com/science/article/pii/S0168192314002123, 2014.

Hudson, R.: Management of Agricultural, Forestry, Fisheries and Rural Enterprise - Volume I, EOLSS Publications, 2009, https://books.google.co.uk/books?id=-eGvCwAAQBAJ, 2009.

ICRISAT: District Level Database Documentation, Tech. rep., International Crops Research Institute for the Semi-Arid Tropics, Hyderabad, 2015.

Iizumi, T. and Ramankutty, N.: How do weather and climate influence cropping area and intensity?, Global Food Security, 4, 46 – 50, https://doi.org/https://doi.org/10.1016/j.gfs.2014.11.003, http://www.sciencedirect.com/science/article/pii/S2211912414000583, 2015.

Jones, R. G., Noguer, M., Hassell, D. C., Hudson, D., Wilson, S. S., Jenkins, G. J., and Mitchell, J. F.: Generating high resolution climate change scenarios using PRECIS, Met Office Hadley Centre, Exeter, UK, pp. 0–40, http://precis.metoffice.com/docs/PRECIS_Handbook.pdf, 2004.

Kumar, P., Wiltshire, A., Mathison, C., Asharaf, S., Ahrens, B., Lucas-Picher, P., Christensen, J. H., Gobiet, A., Saeed, F., Hagemann, S., and Jacob, D.: Downscaled climate change projections with uncertainty assessment over India using a high resolution multi-model approach, Science of The Total Environment, 468-469, Supplement, S18 – S30, https://doi.org/http://dx.doi.org/10.1016/j.scitotenv.2013.01.051, http://www.sciencedirect.com/science/article/pii/S004896971300106X, changing water resources availability in Northern India with respect to Himalayan glacier retreat and changing monsoon patterns: consequences and adaptation, 2013.

Kumar, R., Singh, R., and Sharma, K.: Water resources of India, Current Science, 89, 794–811, 2005.

Laik, R., Sharma, S., Idris, M., Singh, A., Singh, S., Bhatt, B., Saharawat, Y., Humphreys, E., and Ladha, J.: Integration of conservation agriculture with best management practices for improving system performance of the rice–wheat rotation in the Eastern Indo-Gangetic Plains of India, Agriculture, Ecosystems & Environment, 195, 68–82, https://doi.org/https://doi.org/10.1016/j.agee.2014.06.001, http://www.sciencedirect.com/science/article/pii/S0167880914003211, 2014.

Liu, L., Xu, X., Zhuang, D., Chen, X., and Li, S.: Changes in the Potential Multiple Cropping System in Response to Climate Change in China from 1960–2010, PLoS ONE, 8, https://doi.org/https://doi.org/10.1371/JOURNAL.PONE.0080990, http://journals.plos.org/plosone/article/file?id=10.1371/journal.pone.0080990&type=printable, 2013.

Mahajan, A. and Gupta, R. D., eds.: The Rice–Wheat Cropping System, pp. 109–117, Springer Netherlands, Dordrecht, https://doi.org/10.1007/978-1-4020-9875-8_7, https://doi.org/10.1007/978-1-4020-9875-8_7, 2009.

Makino, A.: Rubisco and nitrogen relationships in rice: Leaf photosynthesis and plant growth, Soil Science and Plant Nutrition, 49, 319–327, https://doi.org/10.1080/00380768.2003.10410016, https://doi.org/10.1080/00380768.2003.10410016, 2003.

Mathison, C., Wiltshire, A., Dimri, A., Falloon, P., Jacob, D., Kumar, P., Moors, E., Ridley, J., Siderius, C., Stoffel, M., and Yasunari, T.: Regional projections of North Indian climate for adaptation studies, Science of The Total Environment, 468-469, Supplement, S4–S17, https://doi.org/http://dx.doi.org/10.1016/j.scitotenv.2012.04.066, http://www.sciencedirect.com/science/article/pii/S0048969712006377, 2013.

Mathison, C., Wiltshire, A. J., Falloon, P., and Challinor, A. J.: South Asia river-flow projections and their implications for water resources, Hydrology and Earth System Sciences, 19, 4783–4810, https://doi.org/10.5194/hess-19-4783-2015, http://www.hydrol-earth-syst-sci.net/19/4783/2015/, 2015.

Mathison, C., Deva, C., Falloon, P., and Challinor, A. J.: Estimating sowing and harvest dates based on the Asian Summer Monsoon, Earth System Dynamics, 9, 563–592, https://doi.org/10.5194/esd-9-563-2018, https://www.earth-syst-dynam.net/9/563/2018/, 2018.

Monfreda, C., Ramankutty, N., and Foley, J. A.: Farming the planet: 2. Geographic distribution of crop areas, yields, physiological types, and net primary production in the year 2000, Global Biogeochemical Cycles, 22, https://doi.org/10.1029/2007GB002947, https://agupubs.onlinelibrary.wiley.com/doi/abs/10.1029/2007GB002947, 2008.

Mueller, B., Hauser, M., Iles, C., Rimi, R. H., Zwiers, F. W., and Wan, H.: Lengthening of the growing season in wheat and maize producing regions, Weather and Climate Extremes, 9, 47 – 56, https://doi.org/https://doi.org/10.1016/j.wace.2015.04.001, http://www.sciencedirect.com/science/article/pii/S2212094715000183, the World Climate Research Program Grand Challenge on Extremes – WCRP-ICTP Summer School on Attribution and Prediction of Extreme Events, 2015.

Nicklin, K.: Seasonal crop yield forecasting in semi-arid West Africa, PhD thesis, University of Leeds, 1, Chapter 4, 2012.

Noilhan, J. and Planton, S.: A Simple Parameterization of Land Surface Processes for Meteorological Models, Monthly Weather Review, 117, 536–549, https://doi.org/10.1175/1520-0493(1989)117<0536:ASPOLS>2.0.CO;2, 1989.

Ocheltree, T. W., Nippert, J. B., and Prasad, P. V. V.: Stomatal responses to changes in vapor pressure deficit reflect tissue-specific differences in hydraulic conductance, Plant, Cell & Environment, 37, 132–139, https://doi.org/10.1111/pce.12137, https://onlinelibrary.wiley.com/doi/abs/10.1111/pce.12137, 2014.

Ogbaga, C.: Regulation of Photosynthesis in Sorghum in response to drought, PhD Thesis, University of Manchester, 1, 1–186, https://doi.org/10.13140/RG.2.1.4756.5208, https://www.researchgate.net/profile/Chukwuma_Ogbaga/publication/301364410/inline/jsViewer/5715f74c08ae0f1a39b1b705, 2014.

Olsovska, K., Kovar, M., Brestic, M., Zivcak, M., Slamka, P., and Shao, H. B.: Genotypically Identifying Wheat Mesophyll Conductance Regulation under Progressive Drought Stress, Frontiers in Plant Science, 7, 1111, https://doi.org/10.3389/fpls.2016.01111, https://www.frontiersin.org/article/10.3389/fpls.2016.01111, 2016.

Osborne, T., Gornall, J., Hooker, J., Williams, K., Wiltshire, A., Betts, R., and Wheeler, T.: JULES-crop: a parametrisation of crops in the Joint UK Land Environment Simulator, Geoscientific Model Development, 8, 1139–1155, https://doi.org/10.5194/gmd-8-1139-2015, 2015.

Penning de Vries, F. W. T., Jansen, D., ten Berge, H., and Bakema, A.: Simulation of Ecophysiological Processes of Growth in Several Annual Crops, Simulation monographs, Pudoc, https://books.google.co.uk/books?id=G-cjxJlr71wC, 1989.

Petrie, C. A., Singh, R. N., Bates, J., Dixit, Y., French, C. A. I., Hodell, D. A., Jones, P. J., Lancelotti, C., Lynam, F., Neogi, S., Pandey, A. K., Parikh, D., Pawar, V., Redhouse, D. I., and Singh, D. P.: Adaptation to Variable Environments, Resilience to Climate Change:

Investigating Land, Water and Settlement in Indus Northwest India, Current Anthropology, 58, 1–30, https://doi.org/10.1086/690112, https://doi.org/10.1086/690112, 2017.

Pires, G. F., Abrahão, G. M., Brumatti, L. M., Oliveira, L. J., Costa, M. H., Liddicoat, S., Kato, E., and Ladle, R. J.: Increased climate risk in Brazilian double cropping agriculture systems: Implications for land use in Northern Brazil, Agricultural and Forest Meteorology, 228-229, 286 – 298, https://doi.org/https://doi.org/10.1016/j.agrformet.2016.07.005, http://www.sciencedirect.com/science/article/pii/S0168192316303318, 2016.

Portmann, F. T., Siebert, S., and Döll, P.: MIRCA2000-Global monthly irrigated and rainfed crop areas around the year 2000: A new high-resolution data set for agricultural and hydrological modeling, Global Biogeochemical Cycles, 24, n/a–n/a, https://doi.org/10.1029/2008GB003435, http://dx.doi.org/10.1029/2008GB003435, gB1011, 2010.

Ramankutty, N., Evan, A. T., Monfreda, C., and Foley, J. A.: Farming the planet: 1. Geographic distribution of global agricultural lands in the year 2000, Global Biogeochemical Cycles, 22, n/a–n/a, https://doi.org/10.1029/2007GB002952, http://dx.doi.org/10.1029/2007GB002952, 2008.

Ray, D. K., Ramankutty, N., and and, N. D. M.: Recent patterns of crop yield growth and stagnation., Nature Communications, 3, 1293–1300, https://doi.org/10.1038/ncomms2296, 2012a.

Ray, D. K., Ramankutty, N., Mueller, N. D., West, P. C., and Foley, J. A.: Harvested Area and Yield for 4 Crops (1995-2005), http://www.earthstat.org/harvested-area-yield-4-crops-1995-2005/, 2012b.

Rivington, M. and Koo, J.: Report on the Meta-Analysis of Crop Modelling for Climate Change and Food Security Survey, Climate Change, Agriculture and Food Security Challenge Program of the CGIAR, https://cgspace.cgiar.org/rest/bitstreams/9114/retrieve, 2010.

Robertson, M., Brooking, I., and Ritchie, J.: Temperature Response of Vernalization in Wheat: Modelling the Effect on the Final Number of Mainstem Leaves, Annals of Botany, 78, 371–381, https://doi.org/10.1006/anbo.1996.0132, 1996.

Rosenzweig, C., Jones, J., Hatfield, J., Ruane, A., Boote, K., Thorburn, P., Antle, J., Nelson, G., Porter, C., Janssen, S., Asseng, S., Basso, B., Ewert, F., Wallach, D., Baigorria, G., and Winter, J.: The Agricultural Model Intercomparison and Improvement Project (AgMIP): Protocols and pilot studies, Agricultural and Forest Meteorology, 170, 166 – 182, https://doi.org/http://dx.doi.org/10.1016/j.agrformet.2012.09.011, http://www.sciencedirect.com/science/article/pii/S0168192312002857, agricultural prediction using climate model ensembles, 2013.

Rosenzweig, C., Elliott, J., Deryng, D., Ruane, A. C., Müller, C., Arneth, A., Boote, K. J., Folberth, C., Glotter, M., Khabarov, N., Neumann, K., Piontek, F., Pugh, T. A. M., Schmid, E., Stehfest, E., Yang, H., and Jones, J. W.: Assessing agricultural risks of climate change in the 21st century in a global gridded crop model intercomparison, Proceedings of the National Academy of Sciences, 111, 3268–3273, https://doi.org/10.1073/pnas.1222463110, http://www.pnas.org/content/111/9/3268.abstract, 2014.

Sacks, W. J., Deryng, D., Foley, J. A., and Ramankutty, N.: Crop planting dates: an analysis of global patterns, Global Ecology and Biogeography, 19, 607–620, 2010.

Shannon, S., Smith, R., Wiltshire, A., Payne, T., Huss, M., Betts, R., Caesar, J., Koutroulis, A., Jones, D., and Harrison, S.: Global glacier volume projections under high-end climate change scenarios, The Cryosphere Discussions, 2018, 1–36, https://doi.org/10.5194/tc-2018-35, https://www.the-cryosphere-discuss.net/tc-2018-35/, 2018.

Sharma, B. and Sharma, H.: Status of Rice Production in Assam, India, Journal of Rice Research: Open Access, 3, 3–e121, https://doi.org/10.4172/2375-4338.1000e121, https://www.omicsonline.org/open-access/status-of-rice-production-in-assam-india-2375-4338-1000121.pdf, 2015.

Simmons, A., Uppala, S., Dee, D., and Kobayashi, S.: ERA-Interim: New ECMWF reanalysis products from 1989 onwards., ECMWF Newsletter - Winter 2006/07, 110, 25–35, 2007.

Sinclair, T., Jr, P. P., Kimball, B., Adamsen, F., LaMorte, R., Wall, G., Hunsaker, D., Adam, N., Brooks, T., Garcia, R., Thompson, T., Leavitt, S., and Matthias, A.: Leaf nitrogen concentration of wheat subjected to elevated [CO2] and either water or N deficits, Agriculture, Ecosystems & Environment, 79, 53 – 60, https://doi.org/https://doi.org/10.1016/S0167-8809(99)00146-2, http://www.sciencedirect.com/science/article/pii/S0167880999001462, 2000.

Tuinenburg, O. A., Hutjes, R. W. A., Stacke, T., Wiltshire, A., and Lucas-Picher, P.: Effects of irrigation in india on the atmospheric water budget., Journal of Hydrometeorology, 15, 1028–1050, https://doi.org/10.1175/JHM-D-13-078.1, 2014.

Waha, K., van Bussel, L. G. J., Müller, C., and Bondeau, A.: Climate-driven simulation of global crop sowing dates, Global Ecology and Biogeography, 21, 247–259, https://doi.org/10.1111/j.1466-8238.2011.00678.x, http://dx.doi.org/10.1111/j.1466-8238.2011.00678.x, 2012.

Waha, K., Müller, C., Bondeau, A., Dietrich, J., Kurukulasuriya, P., Heinke, J., and Lotze-Campen, H.: Adaptation to climate change through the choice of cropping system and sowing date in sub-Saharan Africa, Global Environmental Change, 23, 130 – 143, https://doi.org/https://doi.org/10.1016/j.gloenvcha.2012.11.001, http://www.sciencedirect.com/science/article/pii/S095937801200132X, 2013.

Wang, E., Martre, P., Zhao, Z., Ewert, F., Maiorano, A., Rötter, R. P., Kimball, B. A., Ottman, M. J., Wall, G. W., White, J. W., Reynolds, M. P., Alderman, P. D., Aggarwal, P. K., Anothai, J., Basso, B., Biernath, C., Cammarano, D., Challinor, A. J., Sanctis, G. D., Doltra, J., Dumont, B., Fereres, E., Garcia-Vila, M., Gayler, S., Hoogenboom, G., Hunt, L. A., Izaurralde, R. C., Jabloun, M., Jones, C. D., Kersebaum, K. C., Koehler, A.-K., Liu, L., Müller, C., Kumar, S. N., Nendel, C., O'Leary, G., Olesen, J. E., Palosuo, T., Priesack, E., Rezaei, E. E., Ripoche, D., Ruane, A. C., Semenov, M. A., Shcherbak, I., Stöckle, C., Stratonovitch, P., Streck, T., Supit, I., Tao, F., Thorburn, P., Waha, K., Wallach, D., Wang, Z., Wolf, J., Zhu, Y., and Asseng, S.: The uncertainty of crop yield projections is reduced by improved temperature response functions, Nature Plants, 3, 2017.

Warszawski, L., Friend, A., Ostberg, S., Frieler, K., Lucht, W., Schaphoff, S., Beerling, D., Cadule, P., Ciais, P., Clark, D. B., Kahana, R., Ito, A., Keribin, R., Kleidon, A., Lomas, M., Nishina, K., Pavlick, R., Rademacher, T. T., Buechner, M., Piontek, F., Schewe, J., Serdeczny, O., and Schellnhuber, H. J.: A multi-model analysis of risk of ecosystem shifts under climate change, Environmental Research Letters, 8, 044 018, http://stacks.iop.org/1748-9326/8/i=4/a=044018, 2013.

Warszawski, L., Frieler, K., Huber, V., Piontek, F., Serdeczny, O., and Schewe, J.: The Inter-Sectoral Impact Model Intercomparison Project (ISI-MIP): Project framework, Proceedings of the National Academy of Sciences, 111, 3228–3232, https://doi.org/10.1073/pnas.1312330110, http://www.pnas.org/content/111/9/3228.abstract, 2014.

Williams, K., Gornall, J., Harper, A., Wiltshire, A., Hemming, D., Quaife, T., Arkebauer, T., and Scoby, D.: Evaluation of JULES-crop performance against site observations of irrigated maize from Mead, Nebraska, Geoscientific Model Development, 10, 1291–1320, https://doi.org/10.5194/gmd-10-1291-2017, https://www.geosci-model-dev.net/10/1291/2017/, 2017.

Williams, K. E. and Falloon, P. D.: Sources of interannual yield variability in JULES-crop and implications for forcing with seasonal weather forecasts, Geoscientific Model Development Discussions, 8, 4599–4621, https://doi.org/10.5194/gmdd-8-4599-2015, http://www.geosci-model-dev-discuss.net/8/4599/2015/, 2015.

Williams, K. E., Harper, A. B., Huntingford, C., Mercado, L. M., Mathison, C. T., Falloon, P. D., Cox, P. M., and Kim, J.: Revisiting the First ISLSCP Field Experiment to evaluate water stress in JULESv5.0, Geoscientific Model Development Discussions, 2018, 1–47, https://doi.org/10.5194/gmd-2018-210, https://www.geosci-model-dev-discuss.net/gmd-2018-210/, 2018.

Xue, W.: Evaluation of biophysical factors driving temporal variations in C gain, water use and yield production in Rice, PhD thesis, Department of Plant Ecology, University of Bayreuth, 1, 1–230, https://www.researchgate.net/publication/295562013_Evaluation_of_biophysical_factors_driving_temporal_variations_in_carbon_gain_water_use_and_yield_production_in_rice, 2015.

Zhang, G., Dong, J., Zhou, C., Xu, X., Wang, M., Ouyang, H., and Xiao, X.: Increasing cropping intensity in response to climate warming in Tibetan Plateau, China, Field Crops Research, 142, 36 – 46, https://doi.org/https://doi.org/10.1016/j.fcr.2012.11.021, http://www.sciencedirect.com/science/article/pii/S0378429012004091, 2013.

Flag	**JULES notation**	**Avignon settings**	**India settings**	**Effect of switch**
Canopy radiation scheme	can_rad_mod	6	6	Selects the canopy radiation scheme.
Irrigation demand	l_irrig_dmd	F	T	Switches on irrigation demand.
Irrigation scheme	irr_crop	-	2	Irrigation occurs when the DVI of the crop is greater than 0.
Physiology	l_trait_phys	F	F	Switches on trait based physiology when true.
Sowing	l_prescsow	T	T	Selects prescribed sowing.
Plant maintenance respiration	l_scale_resp_pm	F	F	Switch to scale respiration by water stress factor. If false this is leaf respiration only but if true includes all plant maintenance respiration.
Crop rotation	l_croprotate	T	T	A new switch to use the sequential cropping capability.
Irrigation on tiles	frac_irrig_all_tiles	-	F	Switch to allow irrigation on all or specific tiles
Irrigation on specific tiles	set_irrfrac_on_irrtiles	-	T	A new switch to set irrigation to only occur on a specific tile.
Specify irrigated tile(s)	irrigtiles	-	6	Setting to set the value(s) of the specific tile(s) to be irrigated.
Number of tiles irrigated	nirrtile	-	1	Setting to set how many tile(s) to be irrigated.
Set a constant irrigation fraction	const_irrfrac_irrtiles	-	1.0	A new setting to set the value(s) of the irrigation fraction for specific tile(s) to be irrigated in the absence of a file of irrigation fractions.

Table 1. JULES flags used that are new or different from those in Osborne et al. (2015)

Parameter	JULES notation	Description	Winter wheat	Sorghum	Spring wheat	Rice
T_{low}	t_low_io	Lower temperature for photosynthesis (° C).	5	18	5	15
T_{upp}	t_upp_io	Upper temperature for photosynthesis (° C).	30	53	30	40
n_{eff}	neff_io	Scale factor relating V_{cmax} with leaf nitrogen concentration.	0.8e-3	0.75e-3	0.8e-3	0.95e-3
$n_l(0)$	nl0_io	Top leaf nitrogen concentration (kg N/kg C).	0.073	0.07	0.073	0.073
fsmc method	fsmc_mod_io	When equal to 0 we assume an exponential root distribution with depth.			0	0
		When equal to 1, the soil moisture availability factor, fsmc, is calculated using average properties for the root zone.	1	1		
d_r	rootd_ft_io	If fsmc_mod_io = 0 d_r is the e-folding depth.			0.5	0.5
		If fsmc_mod_io = 1 d_r is the total depth of the root zone.	1.5	1.5		
$p0$	fsmc_p0_io	Parameter governing the threshold at which the plant starts to experience water stress due to lack of water in the soil.	0.5	0.5	0.5	0.5
μ_{rl}	nr_nl_io	Ratio of root nitrogen concentration to leaf nitrogen concentration.	0.39	0.39	0.39	0.39
μ_{sl}	ns_nl_io	Ratio of stem nitrogen concentration to leaf nitrogen concentration.	0.43	0.43	0.43	0.43
$Q_{10,leaf}$	q10_leaf_io	Q_{10} factor in the V_{cmax} calculation.	1.0	1.0	1.0	1.0

Table 2. JULES plant functional type (PFT) parameters and values modified for use in this study. We include only the values that have been changed or are new in JULES since Osborne et al. (2015)

Parameter	JULES notation	Description	Winter wheat	Sorghum	Spring wheat	Rice
T_b	t_bse_io	Base temperature (° K).	273.15	284.15	273.15	278.15
T_m	t_max_io	Max temperature (° K).	303.15	317.15	308.15	315.15
T_o	t_opt_io	Optimum temperature (° K).	293.15	305.15	293.15	303.15
TT_{emr}	tt_emr_io	Thermal time between sowing and emergence (° Cd).	35	80	35	60
TT_{veg}	tt_veg_io	Thermal time between emergence and flowering (° Cd).	Table 4	Table 4	Table 5	Table 5
TT_{rep}	tt_rep_io	Thermal time between flowering and maturity (° Cd).	Table 4	Table 4	Table 5	Table 5
T_{mort}	t_mort_io	Soil temperature (2^{nd} level) at which to kill crop if DVI>1 (° K).	273.15	281.15	273.15	281.15
f_{yield}	yield_frac_io	Fraction of the harvest carbon pool converted to yield carbon.	1.0	1.0	1.0	1.0
DVI_{init}	initial_c_dvi_io	DVI at which the crop carbon is set to C_{init}.	0.0	0.0	0.0	0.0
DVI_{sen}	sen_dvi_io	DVI at which leaf senescence begins.	1.5	1.5	1.5	1.5
C_{init}	initial_carbon_io	Carbon in crop at emergence in $\mathrm{kgC/m^2}$.	0.01	0.01	0.01	0.01

Table 3. JULES crop parameters used in this study. The Sorghum cardinal temperatures are from Nicklin (2012) with the other parameters those used for Maize in Osborne et al. (2015). We include only the values that have been changed or added since Osborne et al. (2015). Table 3 of Osborne et al. (2015) provides the original PFT parameters and Table 4 of Osborne et al. (2015) provides the original crop parameters).

Year	Crop	Sowing date	Harvest date	Emergence-flowering	Flowering-maturity	Sowing DOY
2005	Winter wheat	27 Oct 2005		1301.3	867.5	300
2006			27 Jun 2006			
2007	Sorghum	10 May 2007	16 Oct 2007	647.6	791.5	130
2007	Winter wheat	13 Nov 2007		1401.0	934.0	317
2008			1 Jul 2008			
2009	Sorghum	25 Jun 2009	22 Sep 2009	462.5	565.3	176
2009	Winter wheat	19 Nov 2009		1308.6	872.4	323
2010			13 Jul 2010			
2011	Sorghum	22 Apr 2011	22 Sep 2011	679.5	830.5	112
2011	Winter wheat	19 Oct 2011		1559.6	1039.7	292
2012			25 Jun 2012			

Table 4. Thermal times in degree days used in this study for the Avignon site, these are based on the observed sowing and harvest dates from Garrigues et al. (2015).

Location	Crop	Sowing DOY	Emergence-flowering	Flowering-maturity
WestUP	Spring wheat	335	1007.6	671.1
	Rice	150	1759.4	1181.3
EastUP	Spring wheat	335	993.55	662.5
	Rice	150	1865.5	1243.5
WestBi	Spring wheat	335	991.54	661.6
	Rice	150	1907.55	1271.7
EastBi	Spring wheat	335	1019.21	679.1
	Rice	150	1976.96	1300.64

Table 5. The sowing day of year (Sowing DOY) and thermal times in degree days used in this study for the locations in Uttar Pradesh and Bihar, India (see 2 for a map of the locations), the values given here are based on the observed sowing and harvest dates from Bodh et al. (2015)

.

Variable	Simulation type	RMSE	Bias	r value
GPP ($gCm^{-2}day^{-1}$)	AviJUL-grass	2.0	-1.0	0.95
	AviJUL-sqcrop	3.0	0.0	0.82
H (Wm^{-2})	AviJUL-grass	37.0	13.0	0.76
	AviJUL-sqcrop	38.0	6.0	0.71
LE (Wm^{-2})	AviJUL-grass	28.0	-3.0	0.81
	AviJUL-sqcrop	33.0	0.0	0.73

Table 6. Table of statistics comparing the JULES simulations with and without soil moisture prescribed to observations